

Depositional setting and organic matter characterization of the Upper Devonian Antrim Shale, Michigan Basin: Implications for hydrocarbon potential

Ahmed Mansour^{a,*}, Adedoyin Adeyilola^b, Thomas Gentzis^c, Humberto Carvajal-Ortiz^c, Natalia Zakharova^c

^a Geology Department, Faculty of Science, Minia University, Minia, 61519, Egypt

^b Department of Earth and Atmospheric Sciences, Central Michigan University, Mount Pleasant, MI, 48859, United States

^c Core Laboratories, Reservoir Geology Group, 6316 Windfern Road, Houston, TX, 77040, United States

ARTICLE INFO

Keywords:

Palynofacies analysis
Source rock assessment
Prasinophytes
Acritarchs
Frasnian-Famennian
Antrim shale
Michigan basin

ABSTRACT

During the Late Devonian, the Michigan Basin in the Eastern Interior Seaway was characterized by phases of well-developed bottom water anoxia, triggering extensive accumulation of organic matter-rich black shales. Palynological analysis for paleoenvironmental reconstruction and biostratigraphy of the Upper Devonian rocks has been previously performed in other basins of eastern North America, but it is lacking in the Michigan Basin. Here, the Upper Devonian Antrim Shale Formation is investigated for biostratigraphic, paleoenvironmental, and sea level reconstructions, organic matter characterization, and source rock potential. 35 core samples from three drill holes across the Michigan Basin spanning the Norwood, Paxton, Lachine, and Upper members. Palynological analysis showed a moderately diverse assemblage of 31 genera represented by 53 species of relatively well-preserved prasinophyte phycococci and acritarchs, with sparse records of plant spores and freshwater algae. Based on marker prasinophytes and acritarchs, an age of late Frasnian was assigned to the Norwood and Paxton members, while an early Famennian age was proposed to the Lachine and Upper members of the Antrim Shale. Two palynofacies assemblages (PFA) were identified from the variation in the particulate organic matter (POM) composition, both of which indicate deposition in a distal inner neritic shelf environment, but the PFA-2 took place in slightly shallower conditions than the PFA-1. Geochemical screening indicated high organic matter content (up to 25 wt%, avg. 8.5 wt%) and excellent hydrocarbon generating potential of kerogen Type II for the Norwood, Lachine, and Upper members. Only the Paxton Member was dominated by poor to fair organic richness (<0.6 wt%) and low hydrocarbon potential with a mixed Type II/III kerogen. Organic petrography indicated that the dominant organic matter assemblage consists mainly of unicellular marine *Tasmanites* telalginite and *Leiosphaeridia*, followed by solid bitumen of the initial oil type. Thermal maturity, determined from VRo-eq and T_{max}, indicated that all samples are in the oil window, except for some intervals in the Paxton Member.

1. Introduction

Organic matter-rich black to brown shales were broadly deposited throughout the Mid-continental region of North America from southeastern United States to west-central Canada, between the Middle Devonian and Early Mississippian periods (Fig. 1A, Dellapenna, 1991; Ettensohn, 1995; Brown and Kenig, 2004; Formolo et al., 2014). Total organic carbon (TOC) of these sedimentary rocks averages ca. 7 wt% and can reach as high as 25 wt%, particularly in the Appalachian, Michigan,

Illinois, Williston, Ardmore, and Anadarko basins (Nunn et al., 1984; Dellapenna, 1991; Gutschick and Sandberg, 1991; Decker et al., 1992; Martini et al., 1998; Over, 2002; Swezey, 2008; Wei et al., 2016; Liu et al., 2019, 2020). Diverse approaches have been employed to determine the triggering factors of the enhanced organic matter production and preservation in these sediments, including evaluating organic carbon to phosphorous ratio (Ingall et al., 1993), total sulfur to TOC ratio (Leventhal, 1987), trace metals distribution (Werne et al., 2002; Rimmer et al., 2004; Rimmer, 2004; Formolo et al., 2014; Oculalidet et al., 2018;

* Corresponding author.

E-mail address: Ahmedmans48@mu.edu.eg (A. Mansour).

<https://doi.org/10.1016/j.marpetgeo.2022.105683>

Received 4 November 2021; Received in revised form 2 March 2022; Accepted 30 March 2022

Available online 4 April 2022

0264-8172/© 2022 Elsevier Ltd. All rights reserved.

Gilleaudeau et al., 2021), mineral composition (Calvert et al., 1996), and pyrite morphology (Schieber and Baird, 2001). Other studies include organic biomarkers (Brown and Kenig, 2004; Song et al., 2021), and stable isotopes of pyrite sulfur ($\delta^{34}\text{S}_{\text{py}}$) and organic carbon ($\delta^{13}\text{C}_{\text{org}}$, Formolo et al., 2014). These studies suggested different scenarios for environmental changes that controlled enhanced accumulation of organic matter-rich facies. In particular, it remains uncertain if the Laurentia recurrent epeiric seas were subjected to bottom water euxinia during the black shale deposition (Algeo et al., 2007).

Specific examples of these organic matter rich shales include the Upper Devonian Antrim Shale Formation in the Michigan Basin (Fig. 1B) and its age-equivalent units, which are some of the most commercially viable source rock intervals in North America. Previous studies have showed that the Antrim Shale Formation is characterized by deposition of well-preserved, organic carbon-rich, black to brown shale at the top of the Michigan Basin succession (Nunn et al., 1984; Dellapenna, 1991; Decker et al., 1992; Martini et al., 1998; McIntosh et al., 2004; Swezey, 2008; Adeyilola et al., 2022). Formolo et al. (2014) indicated that the boundary between the Paxton and Lachine members of the Antrim Shale Formation in the Michigan Basin coincides with extensive anoxia of the Frasnian-Famennian extinction event (i.e., the Kellwasser Crisis). Thus, the Antrim Shale provides a promising record for better understanding the Late Devonian paleoenvironmental changes, relative richness and evenness of marine phytoplankton and organic carbon accumulations, and their triggering mechanisms in the extensive Eastern Interior Seaway.

In the last few decades, many palynological studies have investigated the palynological composition of microphytoplankton assemblages from the Late Devonian, such as marine prasinophytes, acritarchs, and terrestrially derived plant spores. They provided a comprehensive coverage for the strata in the Appalachian Basin (Winslow, 1962; Wicander, 1975; Jacobson, 1979; Molyneux et al., 1984), the Iowa Basin (Wicander and Playford, 1985), and the Illinois Basin (Bharadwaj et al., 1970; Jacobson, 1979; Wicander, 1983; Huysken et al., 1992; Wicander

and Playford, 2013). However, detailed analysis of palynological composition and palynofacies on the Devonian Antrim Shale Formation from the Michigan Basin, are lacking. Such analysis would allow evaluating the diversity of microphytoplankton assemblages in this stratigraphic interval and describing paleoenvironmental conditions in terms of proximal-distal trends, transgressive-regressive phases, and related sea level changes, as well as determining characteristics of organic matter kerogen types (e.g., Powell et al., 1982; Harker et al., 1990; Tyson, 1993, 1995; Pittet and Gorin, 1997; Mansour et al., 2020a, 2020b, 2020c; Xia et al., 2021).

Palynofacies refers to all particulate organic matter (POM) preserved in sediments, such as phytoclast woody particles, amorphous organic matter (AOM), and palynomorphs. However, palynofacies alone cannot discriminate the hydrocarbon generation potential of organic matter. As such, an integrated approach of palynofacies analysis along with geochemical screening and organic petrographic description is highly recommended for a reliable source rock assessment. Therefore, the present study focuses on a more detailed characterization of the organic matter origin and composition for a better understanding of the source rock intervals and their hydrocarbon potential within the Michigan Basin. In this context, geochemical analyses of Rock-Eval pyrolysis and TOC as well as organic petrography characteristics yield a coherent and precise description of the organic matter quality, quantity, ability to flow hydrocarbons, and degree of thermal maturity (Peters, 1986; Peters et al., 1994; Baskin, 1997; Carvajal-Ortiz and Gentzis, 2015, 2018; Petersen et al., 2020; Mansour et al., 2020a, 2020b; Xia et al., 2021). A few earlier studies have focused on the Antrim Shale's organic and inorganic geochemical characterization, thermal maturity, and isotope geochemistry (e.g., Dellapenna, 1991; Rullkötter et al., 1992; Curtis, 2002; Brown and Kenig, 2004; Swezey, 2008; East et al., 2012; Formolo et al., 2014), but palynofacies investigations and comparison with organic geochemical characterization are sparse.

Therefore, this study presents an integrated approach between various palynological and palynofacies parameters, Rock-Eval pyrolysis

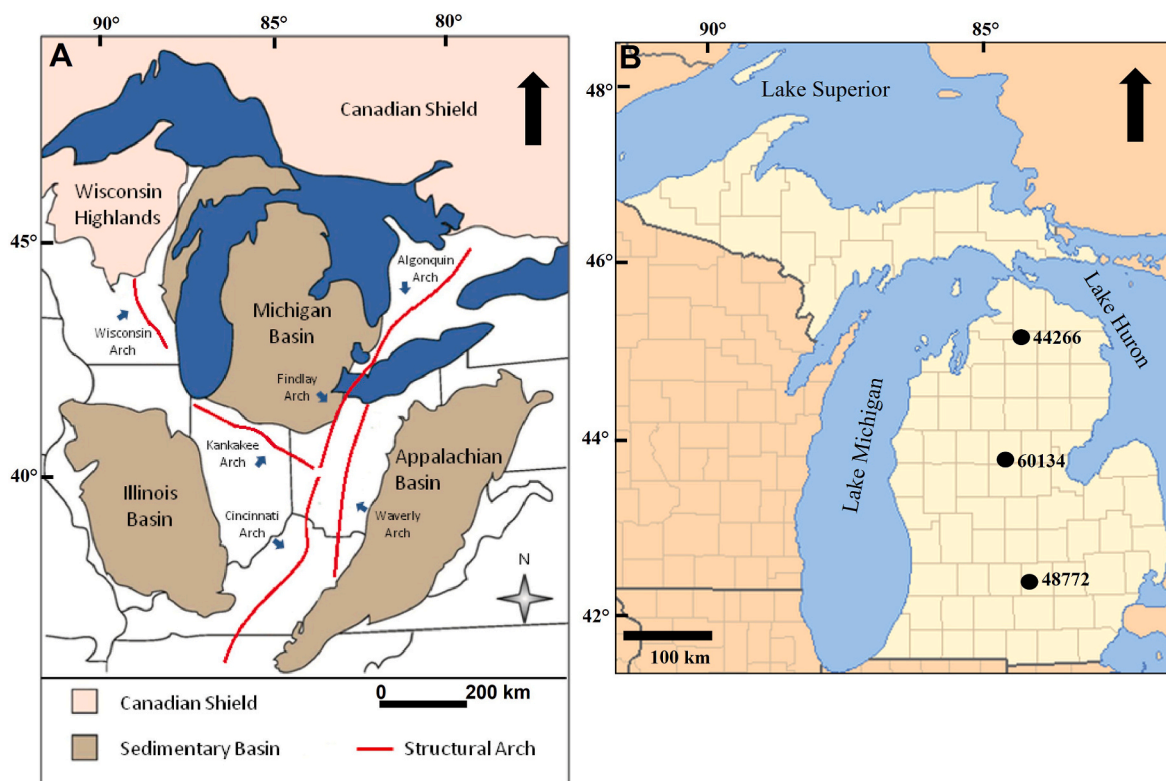


Fig. 1. A) Regional geology map of the Michigan Basin and some tectonic features (modified from Boothroyd, 2012; Structural arches are from Root and Onasch, 1999). B) Location map of the sampled wells in the Michigan Basin (the numbers indicate drill hole permit numbers).

analyses, and organic petrography. The main objectives are to (1) assess the age of deposition of the Norwood, Paxton, Lachine, and Upper members of the Antrim Shale Formation and reconstruct their paleo-environmental conditions based on palynofacies analysis, preserved marine microphytoplankton, and terrestrial palynomorphs, and (2) to evaluate the organic matter quantity, quality, thermal maturity, and its potential to generate and flow hydrocarbons.

2. Geologic settings

The Mid-continent region of the USA is characterized by several giant sedimentary basins, including the Illinois, Michigan, and Appalachian basins (Fig. 1A). The Michigan Basin is an ellipsoidal, intra-cratonic basin, which straddled the Eastern Interior Seaway and was formed by the successive subsidence and deepening during the Paleozoic (Dorr and Eschman, 1970; Nunn et al., 1984). The Michigan Basin (Fig. 1B) is one of the numerous basins associated with low latitude epeiric seas that covered Laurentia paleocontinent during the Devonian period (Formolo et al., 2014). It transitioned from a carbonate shelf depositional environment to a deep basin during the Frasnian because of the effect of the Taghanic Onlap (Johnson, 1970). This event initiated the deposition of the Antrim Shale by raising the sea-level progressively, while the Eastern Interior Seaway subsided at the same time (Gutschick and Sandberg, 1991).

The Michigan Basin is bordered to the east by the Algonquin Arch, to the north by the Canadian Shield, to the south by the KanKakee and Findlay arches and the south Wisconsin lowland. The basin was connected with the adjoining basins to the west through a series of inlets (Fig. 1A, Gutschick and Sandberg, 1991). The Michigan Basin was formed in response to foreland compression and isostatic compensation triggered by the Antler and Acadian orogenies, which controlled the tectonic history and sedimentary processes of the Devonian to Mississippian siliciclastics (Gutschick and Sandberg, 1991). The Michigan Basin is bounded in the northern margin by two major fault systems trending northeast and northwest (Curtis, 2002). These fault systems are marked by thin calcite coatings (Decker et al., 1992; Martini et al., 1998), extending tens of meters in surface exposures of the northern basin margin (Curtis, 2002).

The Michigan Basin was filled with more than 4600 m of sediments, represented by Paleozoic to Mesozoic marine deposits overlaying the Precambrian basement rocks (Fig. 2A). During the Late Ordovician to Late Devonian, the Acadian Orogeny triggered a series of environmental and tectonic events that led to the deposition of fine clastic and carbonate sediments (Quinlan and Beaumont, 1984). At that time, fine siliciclastic sediments started to accumulate in the Appalachian Basin as opposed to enhanced carbonate production in the Michigan Basin, revealing that the active subsidence of the Appalachian Basin might have trapped siliciclastic material from entering the Michigan Basin (Swezey, 2008). During the Late Devonian, fine siliciclastic accumulation extended beyond the Appalachian into the Michigan Basin, thus, fostering the carbonate production collapse and accumulation of the organic-rich Antrim Shale Formation (Fig. 2B, Swezey, 2008). Despite the thick stratigraphic succession of the Antrim Shale Formation across the Michigan Basin, it is laterally absent in the extreme northern and southern margins due to significant truncation by erosion (Dellapenna, 1991). Regionally, the Antrim Shale Formation is stratigraphically equivalent to other black shales deposition in the Eastern Interior Seaway (Chattanooga Shale in the Appalachian Basin, the Bakken Shale in the Williston Basin, and the New Albany Shale in the Illinois Basin, Dellapenna, 1991).

The Antrim Shale Formation is composed of finely laminated to massive, silty, organic-rich and also quartz-rich, black to brown shales and gray calcareous shales (Fig. 2B). The strata of the Michigan Basin dip towards the basin depocenter (Matthews, 1993; McIntosh et al., 2004). The Antrim Shale Formation includes, from oldest to youngest, the Norwood, Paxton, Lachine, and Upper members (Fig. 2B, Gutschick

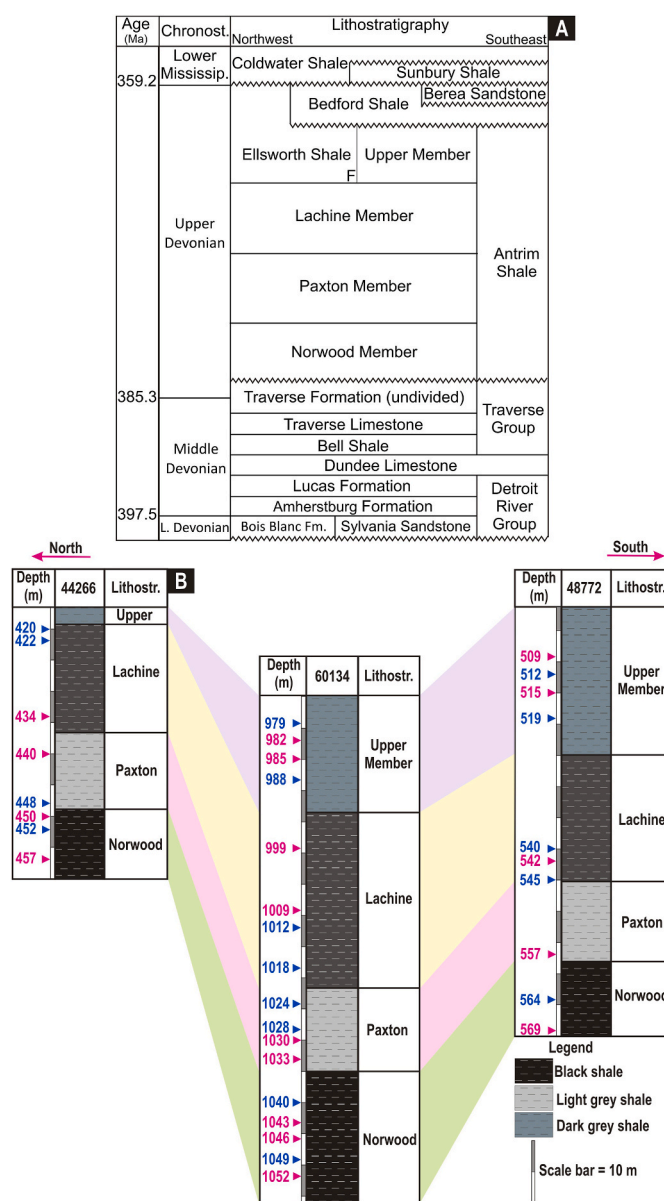


Fig. 2. A) Middle Devonian to Lower Mississippian regional lithostratigraphic chart of the Michigan Basin (modified after Swezey, 2008). B) Lithostratigraphic succession of the Antrim Shale Formation in three drill holes sampled in the Michigan Basin. The 60,134 drill hole represents the basin depocenter, whereas the 44,266 and 48,772 drill holes represent the basin margins relative to north and south directions, respectively. Blue triangles (to the left) define fine samples that were analyzed for geochemistry only, whereas pink triangles signify samples that were processed for both palynology and organic geochemistry analyses in the three drill holes. (For interpretation of the references to color in this figure legend, the reader is referred to the Web version of this article.)

and Sandberg, 1991). The Norwood Member consists of laminated organic matter-rich black shales with minor intercalation of fossiliferous limestone. Quartz content is usually high in this member and reaches up to 50% with plentiful pyrite nodules and calcareous concretions (Dellapenna, 1991). It is overlain by the Paxton Member, which is composed of massive, organic matter-lean, light gray calcareous shale (Gutschick, 1987; Dellapenna, 1991; Martini et al., 1998). The Lachine and the overlying Paxton members are separated by a sharp erosional surface, which corresponds to the extinction event of the late Frasnian (Formolo et al., 2014). The Lachine Member consists of fine lamina composed of quartz and organic-rich brown to black shales. The topmost Upper

Member is an organic-rich unit of black shale, which laterally changes into the Ellsworth Shale in the eastern and central parts of the Michigan Basin (Gutschick and Sandberg, 1991).

3. Materials and methods

3.1. Palynological screening and palynofacies analysis

A total of 18 core samples were collected through the Antrim Shale Formation from three drill holes in the Michigan Basin (Permit Numbers 44,266, 60,134, and 48,772, Fig. 1B). Hole 60,134 is the deepest one, which was drilled in the basin depocenter, in contrast to the other two marginal drill holes (Fig. 2B). The distances of transect between holes 44,266, 60,134, and 48,772 are 117, 134, and 242 km, respectively. The thickness of the Antrim Formation in holes 44,266, 60,134, and 48,772 is 112.5, 169.8, and 65.2 m, respectively. Each member of the Upper, Lachine and Paxton is represented by four samples, except for the Norwood Member, which is represented by 6 samples. Approximately 10 g of each rock sample was crushed into small debris (1–5 mm) and chemically treated using concentrated HCl (34%) and HF (70%) acids following the standard preparation techniques of Wood et al. (1996). The organic residue was sieved in a nylon mesh of 15 µm, followed by permanent mounting on glass slides using Canada Balsam. Chemical treatment using either oxidative nitric acid or alkalis were avoided due to its negative impact on particulate organic matter (POM) composition. Palynological processing of the samples was carried out at the Geology Department, Minia University, Egypt. Two slides were prepared for each sample and examined using a Nikon Eclipse 80i/49 microscope and a ProgRes© SpeedXT^{core} 5 digital camera at the Institute of Paleontology, University of Vienna.

An approximate count of 500 particles of POM, including AOM, opaque and translucent phytoclasts, and palynomorphs, was performed on each sample (Table 1). Stratigraphic variation in the POM composition presents a good opportunity to discriminate between different palynofacies assemblages based on cluster analysis using the Ward's method in the statistical PAST program (Hammer et al., 2001). Additionally, we used the AOM-Phytoclasts-Palynomorphs (APP) ternary plot of Tyson (1993) to tie the cluster analysis to palynofacies results. Also, this ternary diagram is used herein to indicate visual characterization of kerogen composition and types, to reconstruct proximal-distal trends of relative sea level, and to predict changes in terrestrial/riverine

input (e.g., Pittet and Gorin, 1997; Mansour et al., 2020a, 2020b).

3.2. TOC and Rock-Eval pyrolysis

Total organic carbon (TOC) and Rock-Eval pyrolysis analyses were conducted at the Advanced Technology Center, Core Laboratories in Houston, USA. A total of 35 core samples from the above three wells of the Michigan Basin, including samples processed for palynology, were powdered and assessed for their organic matter and hydrocarbon quality, quantity, and thermal maturity (Table 2). All samples were analyzed without solvent extraction. An aliquot of 60 mg of each sample was analyzed by a Rock-Eval® 6 Turbo instrument using one of the IFP Rock-Eval methods®, the Shale Play® method (Romero-Sarmiento et al., 2014; Carvajal-Ortiz and Gentzis, 2018). The advantage of this method is the reliable characterization of source rock intervals of unconventional systems such as fractured, tight, and hybrid shale plays. The initial temperature used to apply this method is 100 °C ± 50 °C (Romero-Sarmiento et al., 2015); however, we used a slightly lower temperature regime of 80 °C to capture any thermo-vaporizable light hydrocarbons remaining in the samples (Carvajal-Ortiz and Gentzis, 2018). The pyrolysis temperature of 80 °C was immediately increased to 200 °C at 25 °C/min. The oven was held isothermal for 3 min at 200 °C to achieve the thermal extraction of the lightest hydrocarbon fraction (Sh0). From 200 °C, the oven temperature increased to 350 °C at a rate of 25 °C/min, staying isothermal at that temperature for 3 min. This was done to achieve thermal extraction of the medium/heavy hydrocarbon fraction or Sh1. The last temperature step consisted of a temperature ramp from 350 °C to 650 °C at 25 °C/min to achieve thermal cracking of the NSO compounds or kerogen fraction, Sh2. The Sh0 and Sh1 fractions are equivalent to the S₁ (free or sorbed hydrocarbons) of the Basic/Bulk-Rock method and Sh2 is equivalent to the S₂ (thermally cracked hydrocarbons indicative of the remaining potential of the organic matter) of the Basic/Bulk-Rock method.

The amounts of CO and CO₂ from thermal decomposition (S₃) and oxidation (S₄) of the organic matter were also obtained. Hydrocarbons and both CO₂ and CO were simultaneously detected via a flame ionization detector (FID for hydrocarbons) and infrared cells (IR cells for CO₂ and CO). All analytical measurements were carried out three times for each sample to check the quality and uniformity of aliquots and to assess analytical precision. Thus, the analytical error for the hydrocarbon pyrolysis parameters (i.e., S₁+S₂) was better than ± 0.5 mg HC/g

Table 1

Particulate organic matter (POM) composition and palynomorphs content of the Antrim Shale samples from the Michigan Basin. Abbreviations; Palynom. = palynomorphs; Transl. = translucent; Equidi. = equidimensional; Opq:Trs = opaque:translucent.

Well name	Member	Sample depth (m)	Total particulate organic matter (POM, 100%)						Total palynomorphs composition (100%)				Opq:Trs ratio	
			AOM	Palynom.	Phytoclasts				Achrirarchs	Prasinophytes	Spores	FWA		
					Total	Transl.	Opagues							
							Lath	Equidi.						
44,266	Lachine	434	87.6	1.7	10.7	2.8	2.8	5.2	36.2	57.5	2.4	3.86	2.9	
	Paxton	440	90.7	0.7	8.5	2.4	3.2	3	40.3	56.3	2.8	0.57	2.6	
	Norwood	450	79	1	20	16.4	0.8	2.8	42.4	51.2	6.4	0	0.2	
		457	88.2	1.7	10	4	2.5	3.5	38.4	52.4	8.1	1.08	1.5	
	60,134	Upper	982	75.2	20.6	4.2	1.2	1	2	18.6	75.6	0.98	4.89	2.5
			985	88.6	1.6	9.8	5.2	1.6	3	41	56.2	2.8	0	0.9
Lachine		999	60.1	3.4	36.5	6.2	8	22.4	27.2	72.8	0	0	4.9	
		1009	70.8	1.4	27.8	4.6	5.2	18.1	29.6	70.4	0	0	5.1	
Paxton		1030	45.2	2	52.8	2	2.4	48.4	31.1	68.9	0	0	25.4	
		1033	51	7.1	41.9	18.5	3.4	20	45.8	49.8	3.5	0.99	1.3	
Norwood		1043	72.2	0	27.8	9.8	5.2	12.8	73.7	21.1	5.3	0	1.8	
		1046	51	2	47	36	3.8	7.2	59.3	37.1	3.6	0	0.3	
1052		59.6	0	40.4	18.4	4.4	17.6	37.3	54.5	0	3.83	1.2		
48,772		Upper	509	86.7	1.4	12	5.4	2.7	3.9	33.9	54.7	11.5	0	1.2
	515		81.9	1.6	16.5	6.8	4.8	5	34.5	56.1	9.5	0	1.4	
	Lachine	542	94.5	1	4.5	0.8	2	1.8	32.3	56.1	11.6	0	4.8	
	Paxton	557	58.3	6.3	35.3	13.7	9.7	11.9	53.1	43.1	3.8	0	1.6	
	Norwood	569	88.8	2	9.2	6.2	2.2	0.8	49.7	47.2	3.1	0	0.5	

Table 2

TOC and Rock-Eval pyrolysis parameters of the Antrim Shale samples measured using the IFP Shale Play method.

Well ID	Member	Depth (m)	TOC	Sh0	Sh1	OIL	Sh2	S3	Tmax	Vro-Eq	HI	OI	PI	OSIs	
			wt%	mg HC/g	mg CO2/g	°C	%	Sh2x100/ TOC	S3x100/ TOC	Oil/(Oil + Sh2)	OILx100/ TOC				
44,266	Lachine	420	5.14	0.94	2.16	3.1	24.59	0.16	435		478.4	3.1	0.11	60.3	
		422	7.4	1.38	2.74	4.12	33.42	0.09	432		451.6	1.2	0.11	55.7	
		434	11.03	2.73	4.33	7.06	55.6	1.24	434	0.71	504.1	11.2	0.11	64.0	
	Paxton	440	0.48	0.05	0.23	0.28	1.16	0.17	438	0.8	241.7	35.4	0.19	58.3	
		448	0.84	0.12	0.82	0.94	3.23	0.2	434		384.5	23.8	0.23	111.9	
	Norwood	450	25.07	2.23	9.79	12.02	116.47	0.86	448	0.74	464.6	3.4	0.09	47.9	
		452	14.85	3.08	5.95	9.03	86.74	0.24	437		584.1	1.6	0.09	60.8	
		457	10.65	2.03	4.03	6.06	63.77	0.23	443	0.75	598.8	2.2	0.09	56.9	
	60,134	Upper	979	1.82	0.34	1.76	2.1	5.61	0.15	441		308.2	8.2	0.27	115.4
			982	2.29	0.55	2.07	2.62	7.16	0.58	443	0.73	312.7	25.3	0.27	114.4
985			3.12	0.51	2.69	3.2	11.53	0.14	443	0.75	369.6	4.5	0.22	102.6	
Lachine		988	3.22	0.89	2.93	3.82	11.73	0.15	442		364.3	4.7	0.25	118.6	
		999	7.42	2.59	4.38	6.97	26.74	0.01	439		360.4	0.1	0.21	93.9	
		1009	8.83	2.69	3.81	6.5	36.83	0.09	441	0.77	417.1	1.0	0.15	73.6	
Paxton		1012	8.76	2.67	3.94	6.61	31.43	0.09	438		358.8	1.0	0.17	75.5	
		1018	9	2.13	3.23	5.36	51.31	0.12	445	0.74	570.1	1.3	0.09	59.6	
		1024	0.58	0.15	0.97	1.12	1.91	0.04	426		329.3	6.9	0.37	193.1	
Norwood		1028	0.59	0.13	0.73	0.86	1.55	0.15	428		262.7	25.4	0.36	145.8	
		1030	0.23	0.07	0.26	0.33	0.6	0.18	426	0.82	260.9	78.3	0.35	143.5	
		1033	1.5	0.42	1.89	2.31	5.36	0.23	435	0.74	357.3	15.3	0.30	154.0	
		1040	14.15	3.76	4.53	8.29	69.11	0.25	439	0.81	488.4	1.8	0.11	58.6	
		1043	10.8	2.92	4.09	7.01	44.48	0.61	442	0.78	411.9	5.6	0.14	64.9	
		1046	1.88	0.34	2.19	2.53	6.89	0.18	432		366.5	9.6	0.27	134.6	
48,772		Upper	1049	12	3.49	4.6	8.09	39.54	0	443	0.82	329.5	0.0	0.17	67.4
			1052	7.49	2.1	3.44	5.54	23.78	0.76	442		317.5	10.1	0.19	74.0
			509	7.86	1.55	2.8	4.35	34.66	0.05	432		441.0	0.6	0.11	55.3
	Lachine	512	5.51	1.17	1.88	3.05	21.52	0.17	431		390.6	3.1	0.12	55.4	
		515	4.56	0.89	1.79	2.68	18.24	0.03	434	0.7	400.0	0.7	0.13	58.8	
		519	6.61	1.34	2.29	3.63	29.75	0.19	436	0.72	450.1	2.9	0.11	54.9	
	Paxton	540	6.47	1.6	2.52	4.12	30.92	0.19	436		477.9	2.9	0.12	63.7	
		542	4.54	1.17	2.23	3.4	20.07	0.25	434		442.1	5.5	0.14	74.9	
		545	8.05	2.23	3.15	5.38	43.13	0.66	436	0.76	535.8	8.2	0.11	66.8	
	Norwood	557	0.29	0.06	0.18	0.24	0.6	0.11	438	0.76	206.9	37.9	0.29	82.8	
564		19.32	4.79	5.66	10.45	110.69	0.15	436	0.77	572.9	0.8	0.09	54.1		
		569	9.9	2.19	3.21	5.4	50.68	0.43	431	0.72	511.9	4.3	0.10	54.5	

rock. Additionally, some calculated parameters were also included, such as hydrogen index ($HI = 100 \times [S_2/TOC]$), oxygen index ($OI = 100 \times S_3/TOC$), production index ($PI = S_1/S_1 + S_2$), and oil saturation index ($OSI = [S_1 \times 100]/TOC$).

3.3. Vitrinite reflectance (Vro-eq)

From the total of 35 samples analyzed by TOC/Rock-Eval pyrolysis, 19 samples were selected for organic petrography analysis. The selection was based on two factors: a) high TOC content, and b) representation from all four members of the Antrim Shale in the three drill holes. An aliquot of 10 g of each sample was milled into ca. 840 μ m, put in the pellets after well-mixing of Epo-Thin epoxy and hardener (2:1, v:v), and left to solidify for 24 h. This was followed by polishing the surface of the pellets using 320 μ m and 600 μ m cloths. Then, alumina powder and water have been used for further polishing with two phases of 0.3 μ m and 0.05 μ m, respectively. Reflected light microscopic investigation using a Zeiss Axiolmager.A2m was carried out at Core Laboratories Inc. in Houston, Texas, USA. The microscopic unit is equipped with digital camera and UV light (fluorescence) source. The UV light investigations were conducted using two filters with an excitation wavelength at 465 nm and a combined beam splitter and barrier filter having a cut at 515 nm. The Yttrium–Aluminum–Garnet (YAG) standard having Ro of 1.0% was used while measuring the random reflectance primary bitumen. Vitrinite Ro-eq was calculated from the measured bitumen Ro values following the equation of Liu et al. (2019). The whole-rock sample preparation method and the reflectance measurements of the organic matter in the Antrim Shale samples were conducted following the ISO standards (ISO 7404-, part 2, 2009; ISO 7404-, part 5, 2009) and ASTM

D7708-14 (2014).

4. Results

4.1. Palynological composition

The Antrim Shale Formation is characterized by a moderate to high palynomorphs recovery of fairly to well-preserved assemblages that are composed mainly of marine-inhabited acritarchs and prasinophyte phycmata (Figs. 3–4). Terrestrially derived plant spores are represented by moderate to low abundance compared to sporadic occurrences of freshwater algae (Fig. 3, Appendix 1). Overall, an assemblage of 31 genera represented by 53 species was defined and counted throughout the studied Antrim Shale samples (Appendix 1). The acritarch assemblage is dominated by *Lophosphaeridium* sp., *L. segregum*, *Comasphaeridium muscosum*, *Alocomurus compactus*, *Micrhystridium* sp., *M. stellatum*, *Veryhachium trispinosum*, *V. europaeum*, *Navifusa bacilla*, and *N. exilis* (Fig. 4). The prasinophyte phycmata includes *Dictyotidium torosum*, *Dictyotidium* sp., *Cymatiosphaera perimembrana*, *C. chelina*, *C. ambotrocha*, *C. parvicarina*, *Leiosphaeridium* sp., *Tasmanites sommeri*, *T. sinuosus*, *Tasmanites* sp., *Muraticavea enteichia*, and *Polyedryxium pharaone*. The pteridophyte plant spores are dominated by trilete spores *Triletes globulus*, *Verrucosporites* sp., *Calamospora obtecta*, *Punctatisporites* sp., *Geminospira lemurata*, and *Cristatisporites cariosus*, and the monolet spore *Laevigatosporites* sp.

4.2. POM composition

For a reliable discrimination of different palynofacies assemblages,

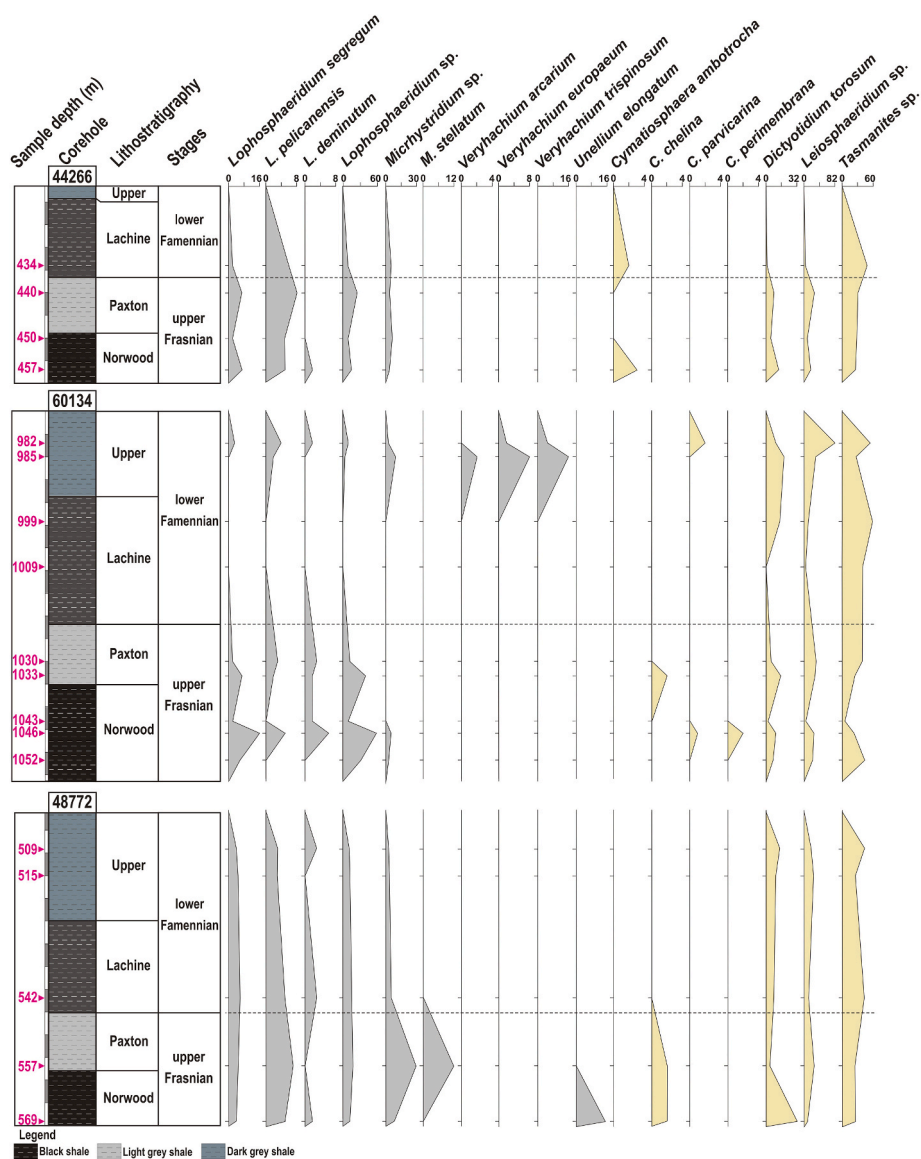


Fig. 3. Stratigraphic distribution chart of recorded acritarchs (gray color) and prasinophytes (light yellow color) from the Upper Devonian Antrim Shale Formation, Michigan Basin. (For interpretation of the references to color in this figure legend, the reader is referred to the Web version of this article.)

all samples of the Antrim Shale Formation were statistically distributed using cluster analysis (Fig. 5A) and then plotted in the APP ternary diagram of Tyson (1993, Fig. 5B). Thus, the studied intervals can be divided into two palynofacies assemblages (PFA) relative to their stratigraphic distribution in the AOM, palynomorphs and phytoclasts contents (Fig. 6). The variation of palynofacies parameters, including equidimensional and lath-shaped opaque wood particles, translucent phytoclasts such as wood tracheid and cuticles, membrane, fungal hyphae, and ratios such as opaque:translucent (Opq:Trs) phytoclasts, and selected palynomorphs are shown in Fig. 6. Samples in the three drill holes under study are largely dominated by AOM (Fig. 7), therefore, each palynofacies assemblage was recognized based on the structured organic matter (i.e., phytoclast content) and the frequency of recovered palynomorphs.

4.2.1. Palynofacies assemblage 1 (PFA-1)

The first PFA is found in most of the Antrim Shale samples in the three drill holes (Figs. 5 and 7). It is dominated by an overwhelming abundance of the AOM (70.8–94.5%, avg. 83.7% of total POM content) compared to low phytoclasts (4.2–27.9%, avg. 13.4% of total POM) and palynomorphs contents (0–20.6%, avg. 2.9% of total POM). The opaque

phytoclasts (3–23.3%, avg. 8% of total POM) have a higher abundance than the translucent woody particles (0.8–16.4%, avg. 5.5%). The equidimensional opaque phytoclasts (0.8–18.1%, avg. 5.2% of total POM) are nearly twice as abundant as the small lath-shaped opaque debris (0.8–5.2%, avg. 2.8%). The Opq:Trs ratio varies widely within the PFA-1 and ranges from 0.2 to 5.1, with an average of 2.1 (Fig. 7). The palynomorphs composition of the PFA-1 is dominated by prasinophyte phycmata (21.1–75.6%, avg. 54.6% of total palynomorphs content (TPC)) followed by acritarchs (18.6–73.7%, avg. 39.2% of TPC). Both groups are regarded as marine phytoplankton. In contrast, terrestrial palynomorphs are also present in the studied samples and are represented by rare to common pteridophyte spores (0–11.6%, avg. 5.3% of TPC) and rare freshwater algae (0–4.9%, avg. 0.9% of TPC).

4.2.2. Palynofacies assemblage 2 (PFA-2)

The second palynofacies cluster is represented by six sample intervals in the drill holes 60,134 and 48,772 (Figs. 5–6). The PFA-2 is dominated by moderate abundances of the AOM (45.2–60.1%, avg. 54.2% of total POM) and phytoclasts (35.3–52.8%, avg. 42.3% of total POM, Fig. 7), with the AOM content showing higher average values than the phytoclast content. The palynomorphs content (0–7.1%, avg. 3.5%

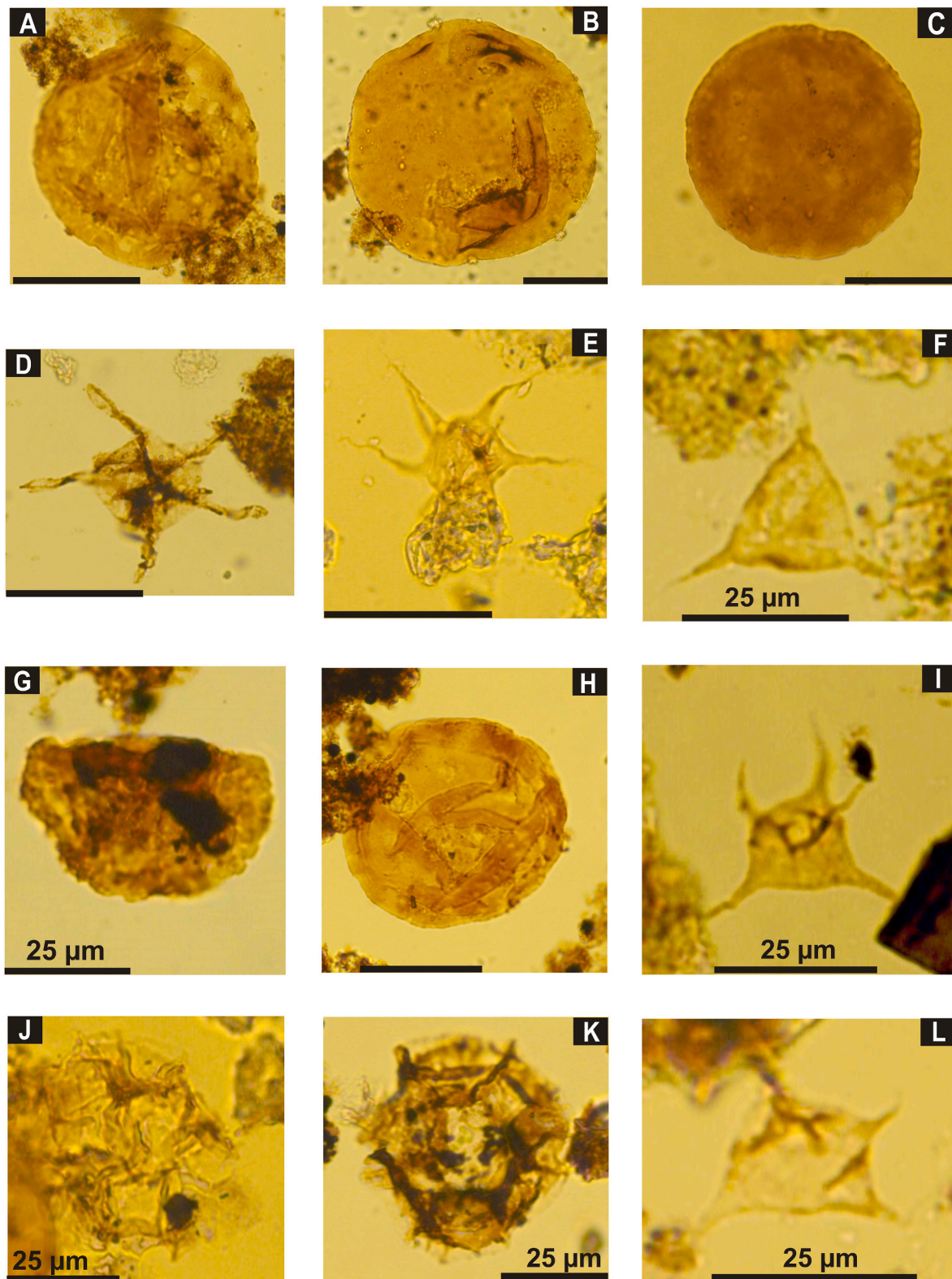


Fig. 4. Microscopic photographs under transmitted white light of recovered palynomorphs from the Antrim Shale Formation, Michigan Basin. The scale bar is ca. 50 μm unless otherwise noted. A) *Tasmanites sinuosus* Winslow (1962), 434 m, Slide A, 44,266 drill hole. B) *Tasmanites sommeri* Winslow (1962), 509 m, Slide A, 48,772 drill hole. C) *Tasmanites* sp., 450 m, Slide A, 44,266 drill hole. D) *Polyedryxium pharaone* Deunff, 1961, 1046 m, Slide B, 60,134 drill hole. E) *Michrystidium* sp. cf. *M. pentagonale* Stockmans and Willièrè, 1963, 557 m, Slide B, 48,772 drill hole. F) *Veryhachium trispinosum* (Eisenack, 1938), Stockmans and Willièrè, 1962, 985 m, Slide A, 60,134 drill hole. G) *Lophosphaeridium deminutum* Playford (1981), 575 m, Slide B, 44,266 drill hole. H) *Leiosphaeridium* sp., 1030 m, Slide A, 60,134 drill hole. I) *Veryhachium europaeum* Stockmans and Willièrè, 1960, 982 m, Slide B, 60,134 drill hole. J) *Cymatiosphaera chelina*, Wicander and Loeblich (1977), 557 m, Slide A, 48,772 drill hole. K) *Cymatiosphaera perimembrana* Staplin, 1961, 1046 m, Slide B, 60,134 drill hole. L) *Veryhachium arcarium*, Wicander and Loeblich (1977), 985 m, Slide B, 60,134 drill hole.

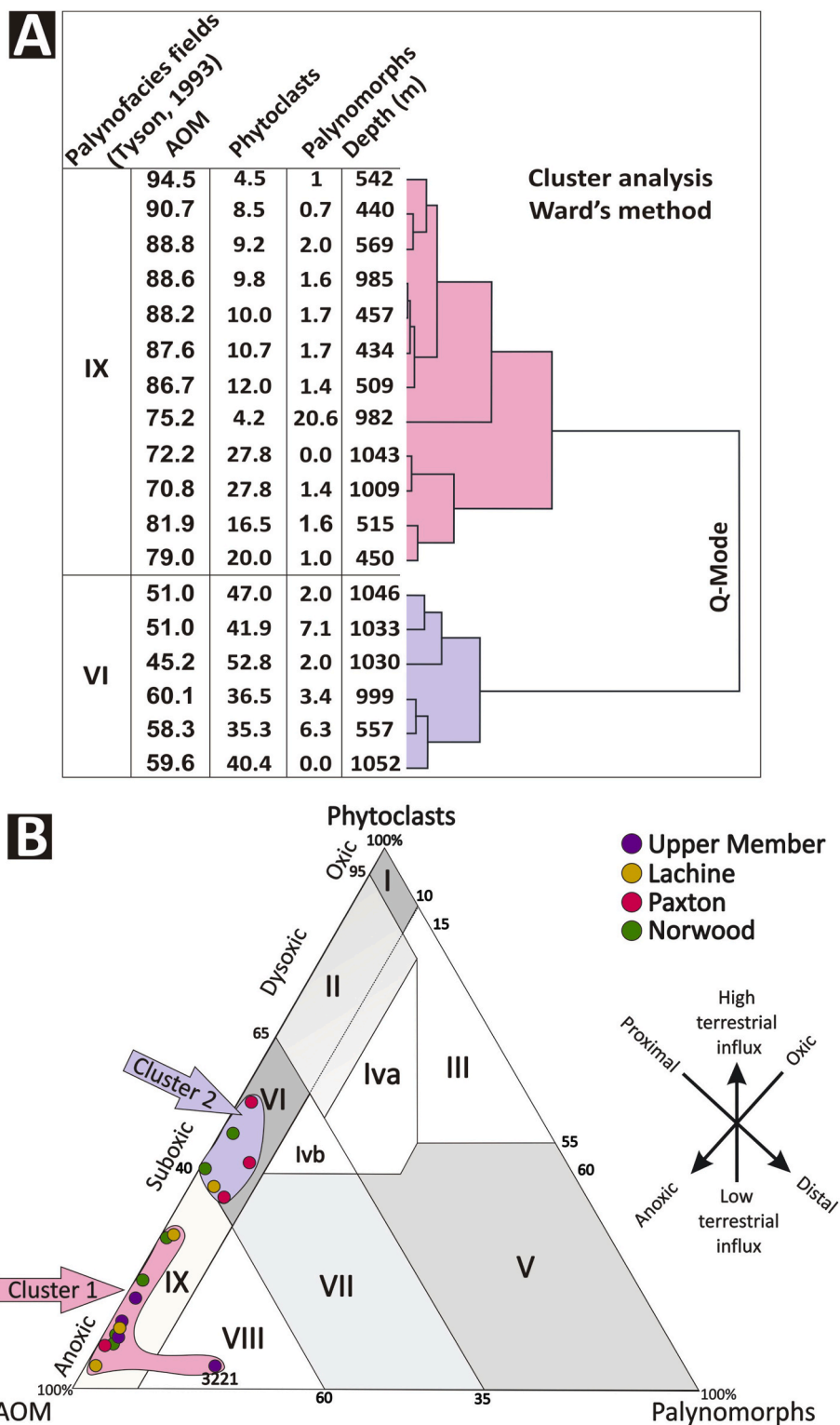


Fig. 5. (A) Statistical analysis of the phytoclasts, AOM, and palynomorphs of the Antrim Shale samples using the Ward's method (Hammer et al., 2001), where all samples are distributed into two clusters that define two different palynofacies assemblages. (B) Ternary diagram of AOM-Phytoclasts-Palynomorphs (after Tyson, 1993) with cluster 1 characterizes the first palynofacies assemblage (PFA-1), while cluster 2 defines the samples of the PFA-2.

of total POM) is considerably lower within the PFA-2. Like PFA-1, the opaque woody particles in the PFA-2 (11–50.8%, avg. 26.5% of total POM) have higher abundance than the translucent wood debris (2–36%, avg. 15.8% of total POM). The amount of equidimensional large opaque wood (7.2–48.4%, avg. 21.3% of total POM) is nearly five times that of the small lath-shaped wood particles (2.4–9.7%, avg. 5.3% of total

POM). Additionally, the Opc:Trs ratio (0.3–25.4, avg. 5.8) is relatively higher in the PFA-2 than in the PFA-1 (Fig. 7). The palynomorph composition of the PFA-2 is similar to the PFA-1, where organic-walled acritarchs (27.2–59.3%, avg. 42.3% of TPC) and prasinophytes (37.1–72.8%, avg. 54.4% of TPC, Figs. 7–8) are the most abundant palynomorph groups. The continental palynomorphs of spores (0–3.8%,

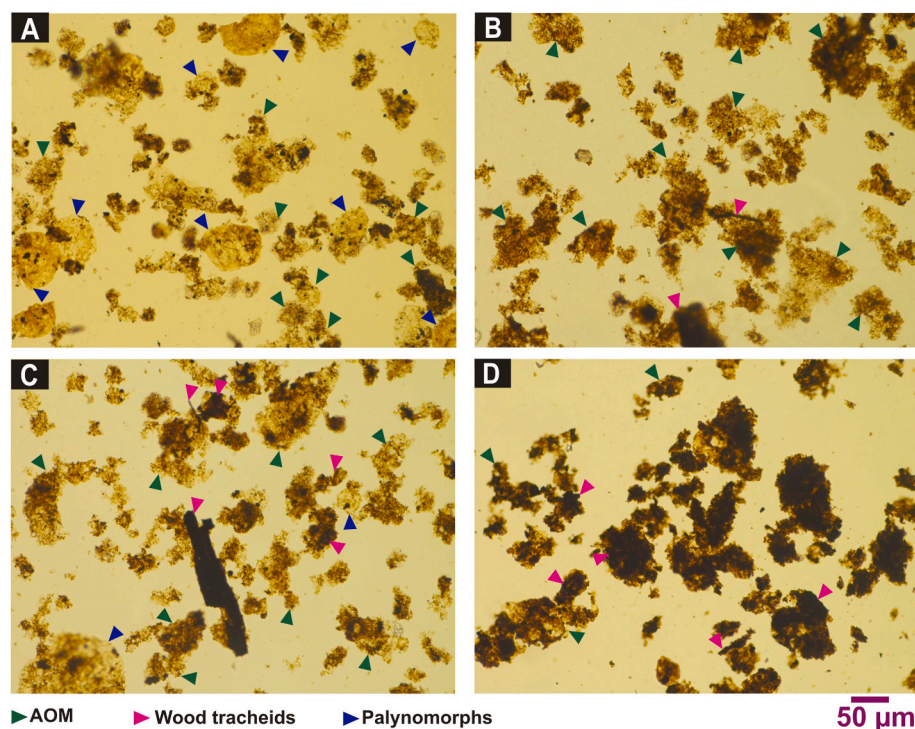


Fig. 6. Microscopic photographs under transmitted white light for POM composition of the Antrim Shale Formation. PFA-1 that composed mainly of AOM recovered from (A) the core sample 3221 of the Upper Member in the 60,134 drill hole, and (B) the core sample 1865 from the Norwood Member in the 48,772 drill hole. (C–D) PFA-2 comprises moderate contents of the AOM and phytoclasts taken from the core sample 1827 and 3379 from the Paxton Member in the 48,772 and 60,134 drill holes, respectively.

avg. 1.8% of TPC) and freshwater algae (0–3.8, avg. 0.8% of TPC) are sparsely recorded within the PFA-2.

4.3. TOC content and Rock-Eval parameters

The TOC and Rock-Eval pyrolysis data are reported in Table 2 and plotted in Fig. 7. The Antrim Shale Formation shows variable quantities and qualities of organic matter. The TOC content has a wide range, from as low as 0.23 wt% (in the Paxton Member) to as high as 25.1 wt%. The highest values of TOC are found in the Norwood Member throughout the three drill holes. The hydrocarbon fractions of S_2 values vary considerably (0.6–116.5 mg HC/g rock, Fig. 9), and the average content is about 32 mg HC/g rock. The HI values range between 207 and 599 mg HC/g TOC, with an average of 409 mg HC/g TOC (Fig. 10), whereas the OI values are notably low to moderate (0–78.3, avg. 9.9 mg CO_2 /g TOC). The maximum temperature of thermal cracking of kerogen (T_{max}) range between 426 and 448 °C (average 437 °C, Fig. 10). The S_1 values are moderate to high (4.5–12 mg HC/g TOC, Fig. 11). The PI is relatively high and reaches up to 0.4 with an average 0.2 (Fig. 12). Lowest S_1 and PI values are recorded within the Paxton Member. The pyrograms of all measured samples displayed a well-developed Gaussian-shaped Sh2 peak (not shown).

4.4. Organic petrography characteristics

Representative photomicrographs taken under reflected white light (RWL) and fluorescent light (FL) along with various organic petrographic characteristics are shown in Figs. 13–15. The dominant organic matter, represented by the green algae *Tasmanites* and *Leiosphaeridia* cysts, accounts for approximately two-thirds of the organofacies population. The remaining one-third is comprised of various types of solid bitumen, rare vitrinite, and some inertinite. The concentration of telalginite and solid bitumen declined in the Upper and Paxton members at the expense of inertinite and vitrinite.

In the 60,134-drill hole, the higher maturity is evident not only by the higher R_o of the solid bitumen and rare vitrinite, but mainly from the weak dull yellow to brown fluorescence colors of the *Tasmanites*

telalginite (Fig. 13). The transformation of *Tasmanites* to bitumen is evident in the Paxton and Upper members (Fig. 13A–G). In the 48,772-drill hole, the solid bitumen R_o is lower and the fluorescence color of *Tasmanites* is golden yellow (Fig. 14C–D, G–L). Here, the Paxton Member contains lower abundance and smaller alginite (Fig. 14I–L) compared to the Norwood (Fig. 14O and P) and Upper members (Fig. 14C and D), which contain thick *Tasmanites*. The Lachine Member contains mostly *Leiosphaeridia* (Fig. 14G and H). Maturity of the organic matter in the 44,266-drill hole in the northern part of the basin is similar to that in the south based on the R_o of the solid bitumen and fluorescence color of *Tasmanites* (Fig. 15). In the northern drill hole, the Paxton Member is poor in alginite, and the algal bodies are small except for rare thick-walled unicellular *Tasmanites* showing the characteristic suture line (Fig. 15E–H).

Solid bitumen in the Antrim Shale was classified following the proposed stages of Sanei (2020). The bitumen reflectance values (BRo) from the Lachine and Norwood black shale members range from 0.53 to 0.70%, and thus, are classified as initial-oil solid bitumen (IOSB). Diagenetic solid bitumen (degraded bituminite with $R_o < 0.5\%$) was seen on one occasion (Paxton Member, drill hole 60,134 at 1033 m).

5. Discussion

5.1. Age diagnostic taxa and correlation

Within the studied samples, monospecific marker taxa exhibit a distinctive biostratigraphic signature for the Antrim Shale Formation (Fig. 3). This includes the *Cymatiosphaera chelina*, *C. perimembrana*, *C. ambotrocha*, *C. parvicarina*, *Lophosphaeridium segregum*, *L. deminutum*, *Veryhachium arcarium*, and *Michhystridium* sp. cf. *M. pentagonale* (Fig. 4). Such taxa give the impression of cosmopolitan marker palynomorphs as they have been broadly recorded in both hemispheres (Winslow, 1962; Bharadwaj et al., 1970; Wicander, 1975, 1983; Wicander and Loeblich, 1977; Playford, 1981; Molyneux et al., 1984; Wicander and Playford, 1985; Li-chang and Wicander, 1988; Huysken et al., 1992; Hashemi and Playford, 1998; Ghavidel-syooki and Owens, 2007; Pereira et al., 2008; Wicander and Playford, 2013). To the best of our knowledge, this is the

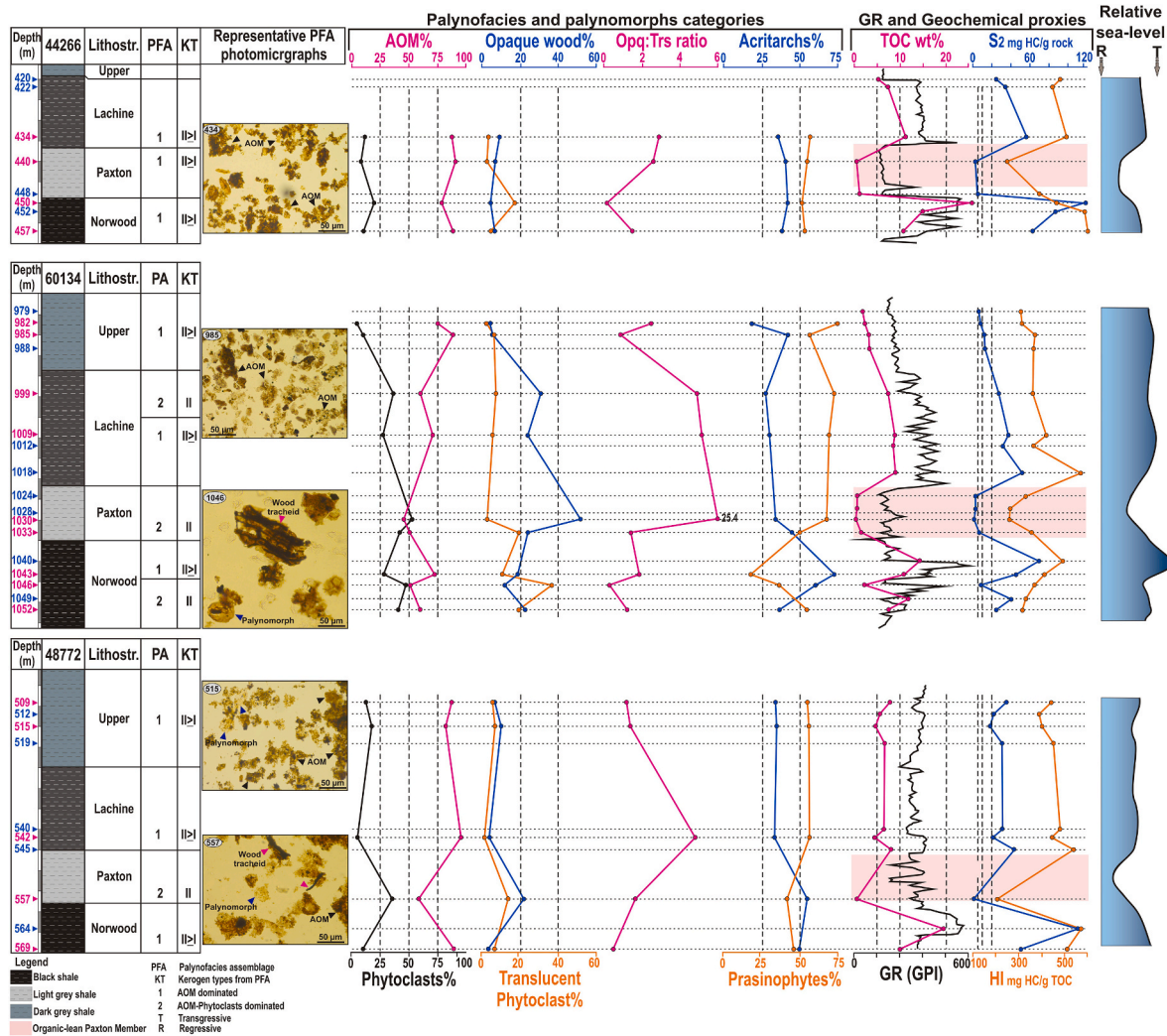


Fig. 7. Stratigraphic vertical composition of various palynofacies and palynomorphs parameters, TOC, and gamma ray log, used to construct relative sea level and environment of deposition of the Upper Devonian Antrim Shale Formation. Percentages of acritarchs and prasinophytes are calculated from total palynomorphs count, while AOM, phytoclasts (opaque and translucent) are of total POM composition. Blue triangles (to the left) define samples that were analyzed for geochemistry only, whereas pink triangles signify samples that were processed for both palynology and organic geochemistry analyses in the three drill holes. (For interpretation of the references to color in this figure legend, the reader is referred to the Web version of this article.)

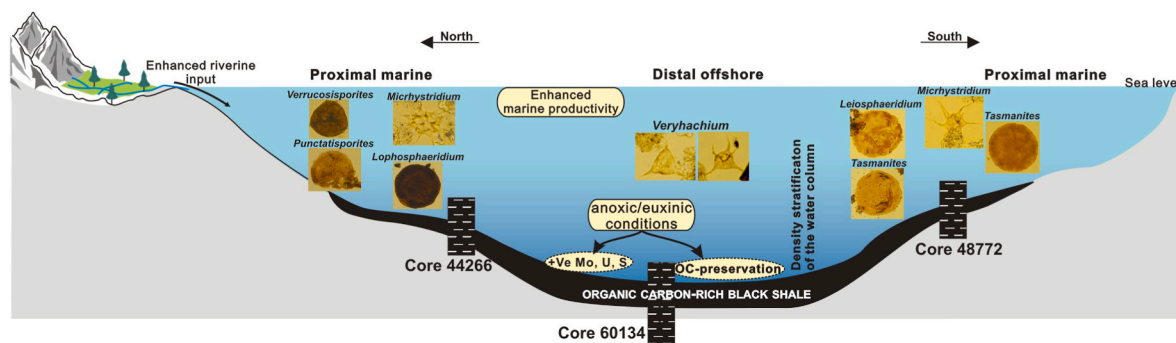


Fig. 8. A schematic model showing possible environmental conditions during deposition of the Upper Devonian Antrim Shale. Representative microscopic photographs of recorded acritarchs, prasinophytes and plant spores in rocks refer to their possible occurrence in a marine environment in the Michigan Basin. Enhanced anoxic-euxinic conditions are observed from palynofacies analysis (this study) and elemental geochemistry of Formolo et al. (2014). The redox conditions illustrated with this model controlled enhanced burial and preservation of organic matter during the deposition of the Norwood and Lachine members.

first detailed palynostratigraphic investigation on the Antrim Shale Formation from the Michigan Basin.

Within the Antrim Shale Formation, the occurrence of the marker

species *Cymatospaera chelina* is restricted to the Norwood and Paxton members, whereas the *C. ambotrocha* is recorded in the Norwood and Lachine members. Additionally, the *C. perimembrana* occurs within the

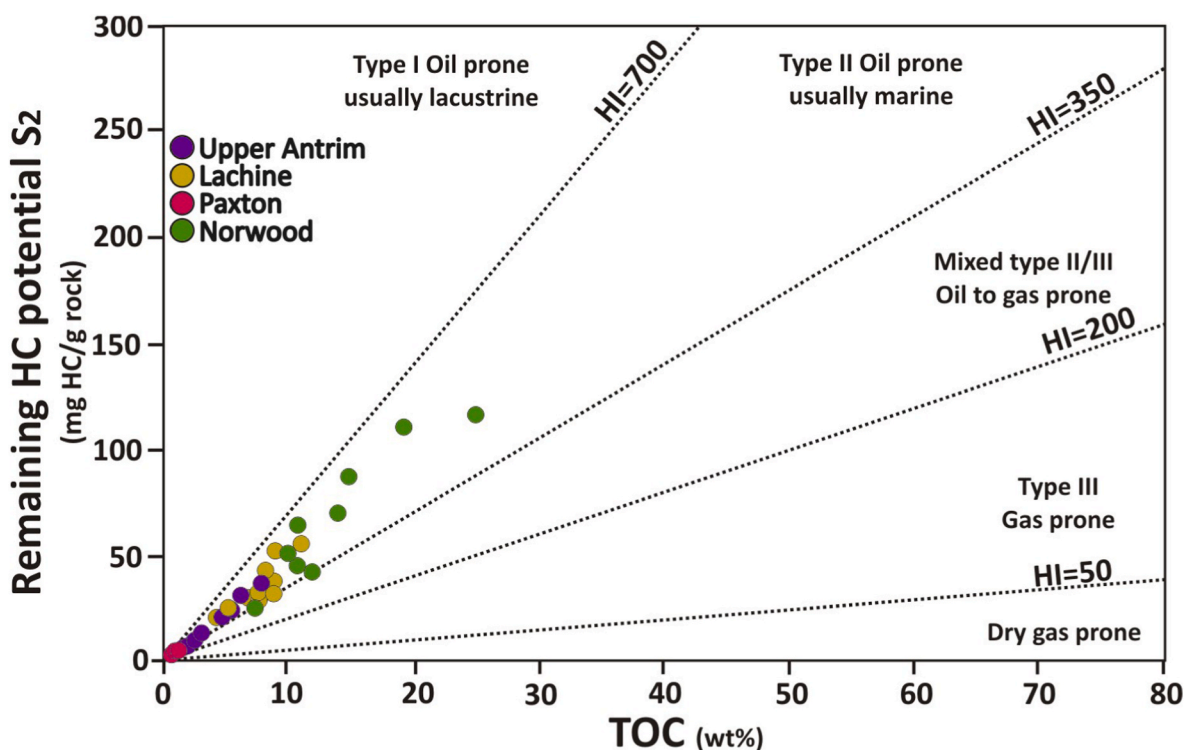


Fig. 9. Plot of the TOC content versus the Rock-Eval S_2 values of the Antrim Shale Formation samples used to indicate kerogen types and source rock generating potential (modified after Langford and Blanc-Valleron, 1990).

Norwood and Upper members, reflecting its occurrence throughout the whole formation compared to the *C. parvicarina* that is reported only within the Norwood Member. *Cymatiosphaera* is one of the most common prasinophyte genera that is widely known to have first appeared within the Late Devonian and to become very frequent particularly within the Frasnian-Famennian time. The *Cymatiosphaera* genus is represented by *C. chelina*, *C. ambotrocha*, and *C. parvicarina*, which were previously documented from the Upper Devonian strata (Frasnian to Famennian) of the Antrim Shale Formation in Indiana (Wicander and Loeblich, 1977), the upper Frasnian-lower Famennian strata of the Lime Creek Formation in the Iowa Basin (Wicander and Playford, 1985), and the Upper Devonian (Famennian) Saverton Shale Formation in the Illinois Basin (Wicander and Playford, 2013). The *C. parvicarina* was also reported from the upper Famennian strata of the Chagrin Shale in Ohio, USA (Wicander, 1974). The *Cymatiosphaera perimembrana* is commonly distributed throughout the Frasnian-Famennian sediments in North America (Iowa and Illinois, Wicander and Playford, 1985; 2013), the southern hemisphere in Western Australia (Western Carnarvon Basin, Playford, 1981), Europe (the South Portuguese Zone, Pereira et al., 2008), and the Middle East (Central Iran Basin, Hashemi and Playford, 1998). Thus, the occurrence of *C. chelina*, *C. ambotrocha*, *C. parvicarina*, and *C. perimembrana* marker prasinophytes within the Antrim Shale Formation suggests an age no younger than Frasnian-Famennian.

The acritarch species *Lophosphaeridium segregum* and *L. deminutum* have a short range and extend from the Frasnian to the Famennian stages. Playford (1981) reported *L. segregum* and *L. deminutum* within the Frasnian Gneudna Formation in Western Australia. Wicander and Playford (1985, 2013) identified *L. segregum* from the upper Frasnian Lime Creek Formation in Iowa and the Saverton Shale Formation in the Illinois Basin, USA. The *L. deminutum* and *L. segregum* were further recorded from the Frasnian-Famennian strata of the Central Iran Basin and the Alborz Mountain in Iran, respectively (Hashemi and Playford, 1998; Ghavidel-syooki and Owens, 2007). These two species are recorded in most samples studied, thus reinforcing an age of Frasnian-Famennian of the Antrim Shale Formation. Wicander (1983)

considered *Veryhachium arcarium* species to mark the late Frasnian-early Famennian transition for sediments of the Antrim Shale Formation in Indiana, USA. Wicander and Playford (1985) assigned the same age based on the common occurrence of the *V. arcarium* within the Lime Creek Formation in Iowa, USA. Additionally, the *V. arcarium* was also reported in the lower Famennian strata of China (Li-chang and Wicander, 1988) and the Frasnian-Famennian Saverton Shale in the USA (Wicander and Playford, 2013). The occurrence of this index taxon was limited only to the Upper Member, which suggests an early Famennian age. This can be further confirmed by previous biostratigraphic assessment of the Upper Member based on the conodont dated *Polygnathus marginifera* zone (Ziegler and Sandberg, 1990).

Overall, we can conclude that marker prasinophyte phycocysts and acritarchs support an age of the Antrim Shale Formation no younger than late Frasnian-early Famennian. Furthermore, based on previously erected conodont dated *Polygnathus linguiformis* and *P. triangularis* zones, Ziegler and Sandberg (1990) assigned an age of late Frasnian and early Famennian to the Paxton and Lachine members, respectively. Thin ash beds (<1 cm) have been reported at the base of the Lachine Member in the Antrim Shale Formation of the Michigan Basin as well as in the age-equivalent Hanover Shale in New York and are commonly identified as the marker beds of the Late Devonian (Frasnian-Famennian) extinction event (Gutschick and Sandberg, 1991; Over, 2002).

5.2. Depositional paleoenvironment

The composition and distribution of POM are physically controlled by ecological and sedimentological processes within the depositional environment. Several palynofacies parameters were utilized for the Antrim Shale intervals, such as AOM, phytoclasts (opaque and translucent wood particles), palynomorphs groups, and Opa:Trs ratio. Successive qualitative and quantitative variations of the POM composition generally, and those parameters particularly, led to the definition of two palynofacies assemblages within the Antrim Shale Formation in the Michigan Basin (Figs. 5 and 7), which are advantageous for a reliable

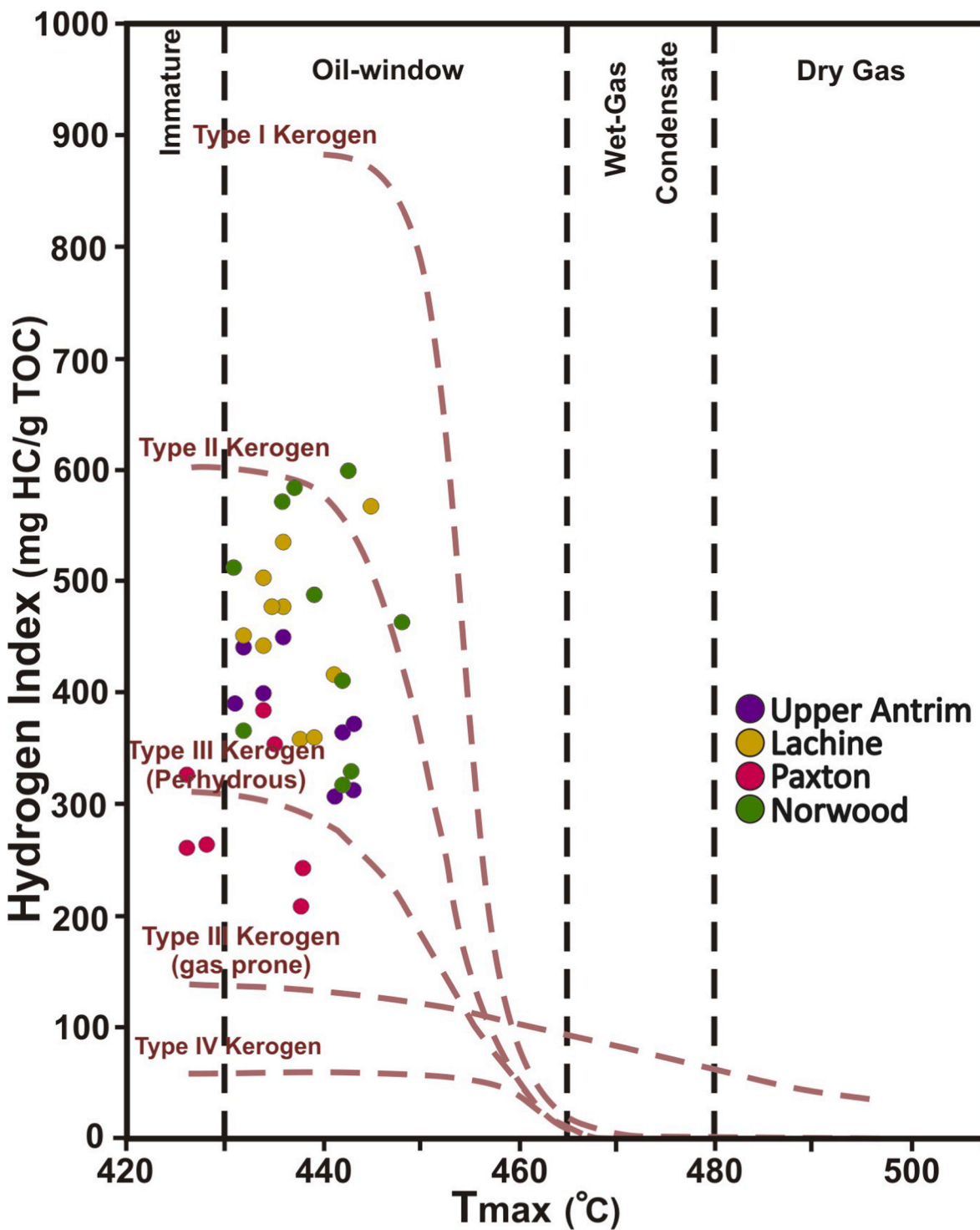


Fig. 10. Relationship between the Rock-Eval HI and T_{max} values of the Antrim Shale samples, used to indicate the degree of thermal maturity and kerogen types (after Espitalié et al., 1985).

reconstruction of the environment of deposition in terms of transgressive-regressive fluctuations of sea level (e.g., Powell et al., 1982; Harker et al., 1990; Tyson, 1993, 1995; Pittet and Gorin, 1997; Mendonça, Filho et al., 2012; Mansour et al., 2020a, 2020b).

5.2.1. PFA-1

The first palynofacies assemblage is dominated by a plethora of the AOM versus very low phytoclasts. Although the TOC content is different between the four members of the Antrim Formation, the PFA-1 occurs in

most samples from the three drill holes (Fig. 5). Differences in TOC contents could be related to physico-chemical processes such as changes in redox conditions triggered by sea level oscillations, biological productivity, riverine inflow, sedimentation rate and preservation conditions (Tyson, 2001; Mansour et al., 2020c).

Here, all samples of PFA-1 plot in the field IX of the APP ternary diagram that defines a highly oil prone kerogen Type II \geq I, except for the sample 982 m from the Norwood Member in the deeper drill hole, which plots in the field VIII due to significantly higher content of

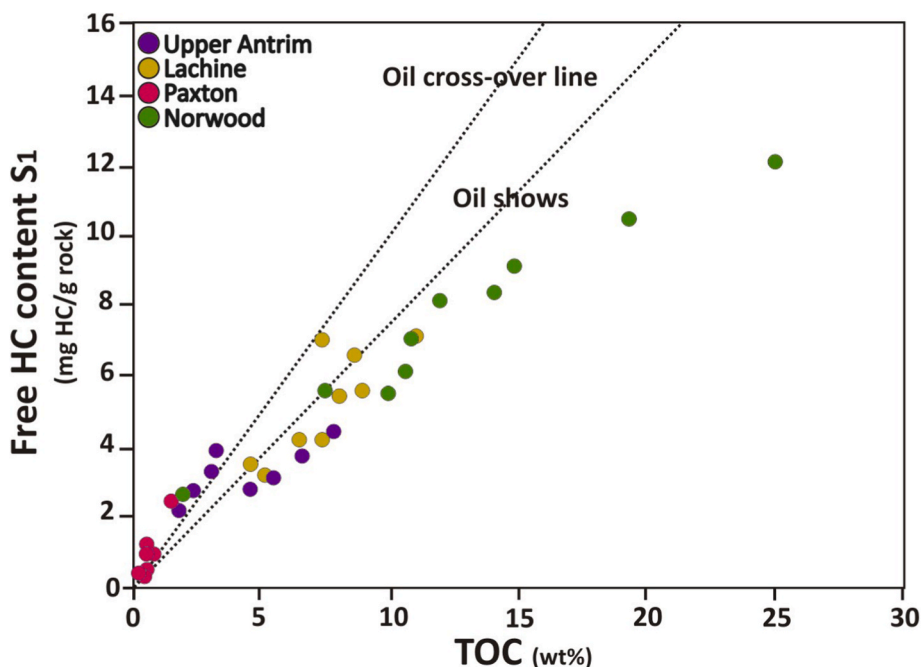


Fig. 11. Relationship between the free hydrocarbon content (Sh₀ + S₁) and TOC values of the Antrim Shale Formation to reveal the possibility of hydrocarbon flow.

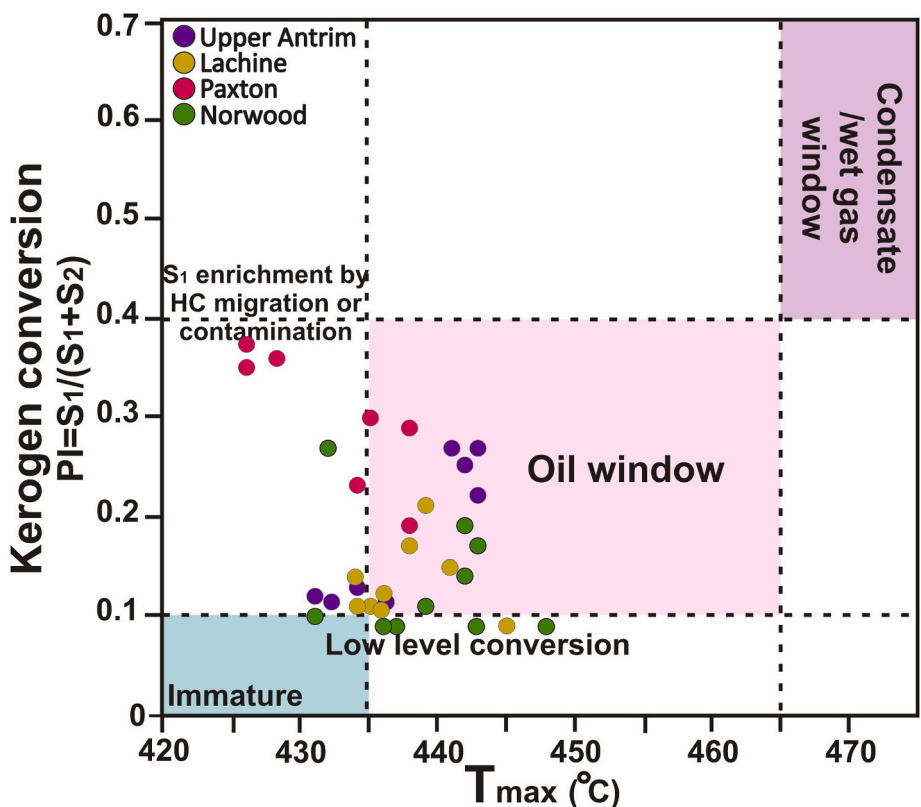


Fig. 12. Cross-plot of the Rock-Eval T_{max} and PI values of the Antrim Shale Formation used to indicate the potential of kerogen conversion to hydrocarbons.

palynomorphs. The latter sample is characterized by oil prone kerogen Type II >> I. The two palynofacies fields of IX and VIII indicate that the samples of the PFA-1 were deposited in a typical sea shelf environment under enhanced water column stratification conditions (e.g., Tyson, 1993, 1995; Mansour et al., 2020a, 2020b, 2020c, Xia et al., 2021). Additionally, both fields reveal deposition under severe anoxic shelf conditions (e.g., Tyson, 1993; Mansour et al., 2020a). Geochemical

investigation of the Antrim Shale showed high pyrite sulfur, Mo, U, Mo/TOC ratio, and a positive trend of δ³⁴S_{py}, revealing deposition of the Lachine and Norwood members under a prevalent euxinic water column (Formolo et al., 2014). Various isorenieratene derivatives were reported in all black shale samples of the Norwood and Lachine members, indicating the predominant occurrence of *Chlorobiaceae* in the water column, and thus, deposition under enhanced euxinia (Brown and Kenig,

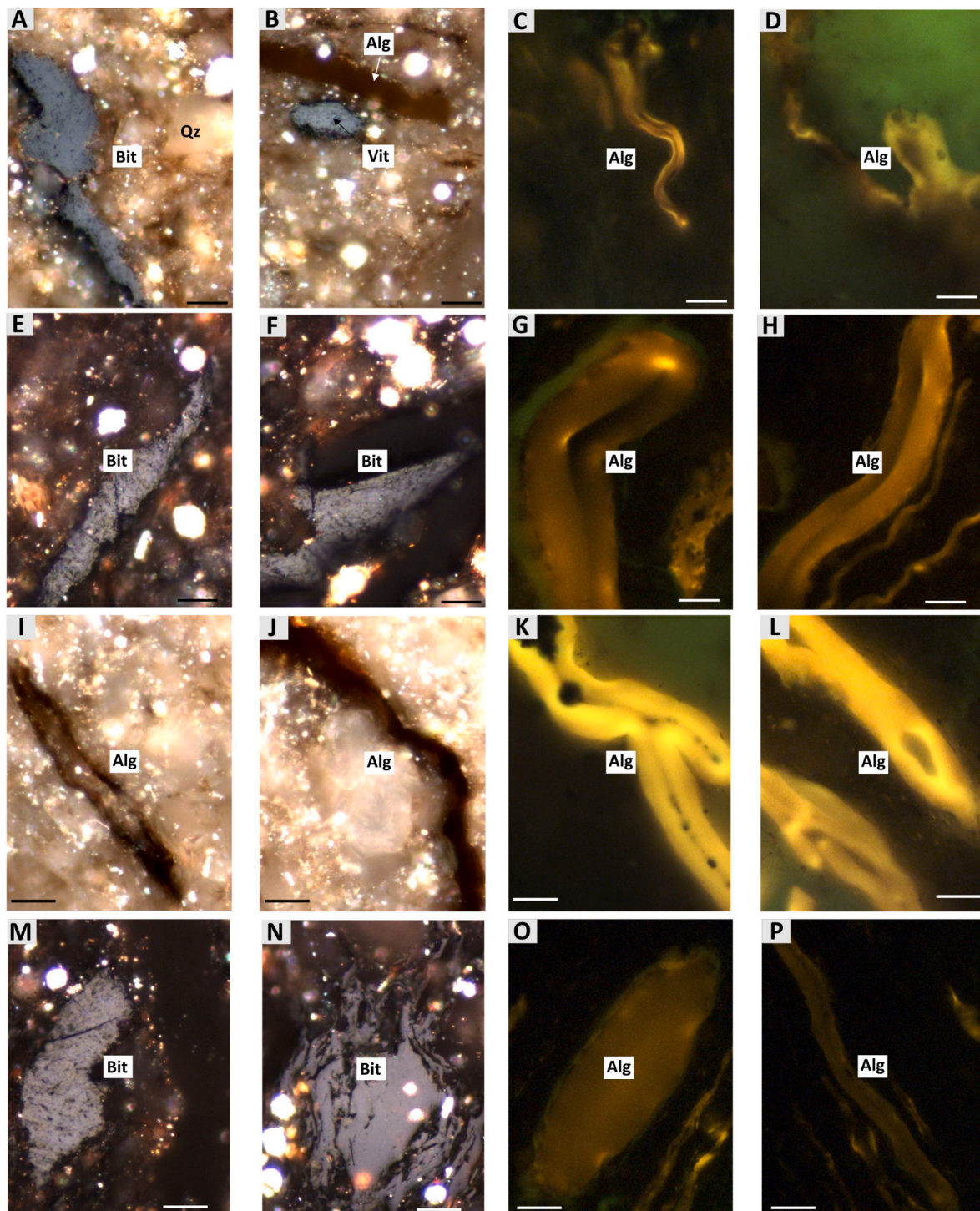


Fig. 13. Photomicrographs of dispersed organic matter from the 60,134 drill hole taken under reflected white light and fluorescence light sources. UV light excitation is at 465 nm; combined dichroic and barrier filter have a cut at 515 nm. The scale bar is 10 μ m. Upper Member at 985 m: (A) Bitumen (BRo = 0.58%), (B) Alginite with primary vitrinite (VRO-eq = 0.73%); Qz = Quartz, (C) Telalginite with dull yellow fluorescence, (D) Telalginite has started to be transformed to bitumen. Lachine Member at 1018 m: (E–F) Bitumen (BRo = 0.67% and 0.62%, respectively), (G–H) *Tasmanites* telalginite showing central suture line and exhibiting dull yellow to light brown fluorescence. Paxton Member at 1033 m; (I–J) Alginite. (K–L) Alginite with mostly dull yellow fluorescence. Norwood Member at 1040 m; (M–N) Bitumen Ro and VRO-eq of 0.64% and 0.71%, respectively, (O–P) Alginite with weak, dull yellow to brown fluorescence. (For interpretation of the references to color in this figure legend, the reader is referred to the Web version of this article.)

2004). Our results from palynofacies fields are consistent with severe reduced conditions of the bottom water; however, palynofacies analysis cannot differentiate between anoxic and euxinic conditions as the latter requires further geochemical proxies (i.e., Mo, U, Cu, Ni, sulfur isotopes, pyrite framboids, etc.). Similar water column redox conditions were also

prevalent during the deposition of age-equivalent intervals from the adjoining Illinois and Appalachian basins (Brown and Kenig, 2004; Rimmer et al., 2004; Rimmer, 2004; Ocubalidet et al., 2018; Gilleaudeau et al., 2021). This suggests that the evolution of the Michigan Basin redox conditions is most likely analogous to the other Late Devonian

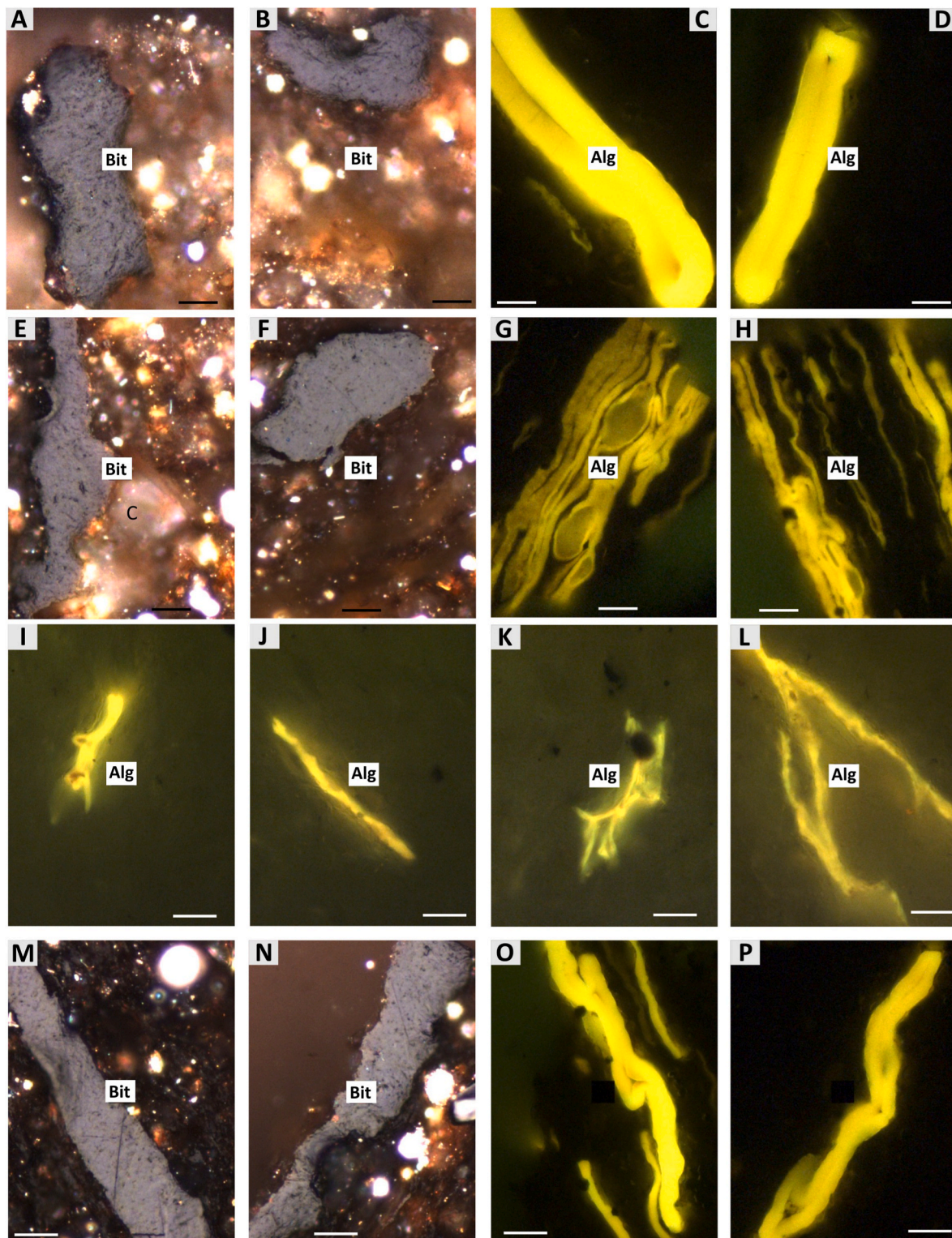


Fig. 14. Photomicrographs of dispersed organic matter from the 48,772 drill hole taken under reflected white light and fluorescence light sources. UV light excitation is at 465 nm; combined dichroic and barrier filter have a cut at 515 nm. The scale bar is 10 μm . Upper Member at 519 m: (A–B) Bitumen BRo of 0.53% and 0.56%, respectively, (C–D) Alginite. Lachine Member at 545 m: (E–F) Bitumen (BRo = 0.54% and 0.58%, respectively), C=Rhombodehral carbonate, (G–H) Alginite. Paxton Member at 557 m: (I–L) Alginite. Norwood Member at 564 m: (M–N) Bitumen BRo of 0.58% and 0.61%, respectively, (O–P) Alginite.

basins in the USA.

The relatively high AOM content within the PFA-1 supports deposition during high sea level in distal shelf environments far from active fluvial sources (Tyson, 1995; Mansour et al., 2020b). Microscopic investigation of the AOM in samples of the PFA-1 reflects a wide variety

of morphologic characteristics, ranging from light yellow to dark brown granular, spongy and/or flaky AOM and gray AOM associated with inclusions of pyrite (Fig. 6, Venkatachala, 1981; Batten, 1996). The former colors of the AOM point to the deposition of the PFA-1 under low-energy conditions in a distal marine environment dominated by well-developed

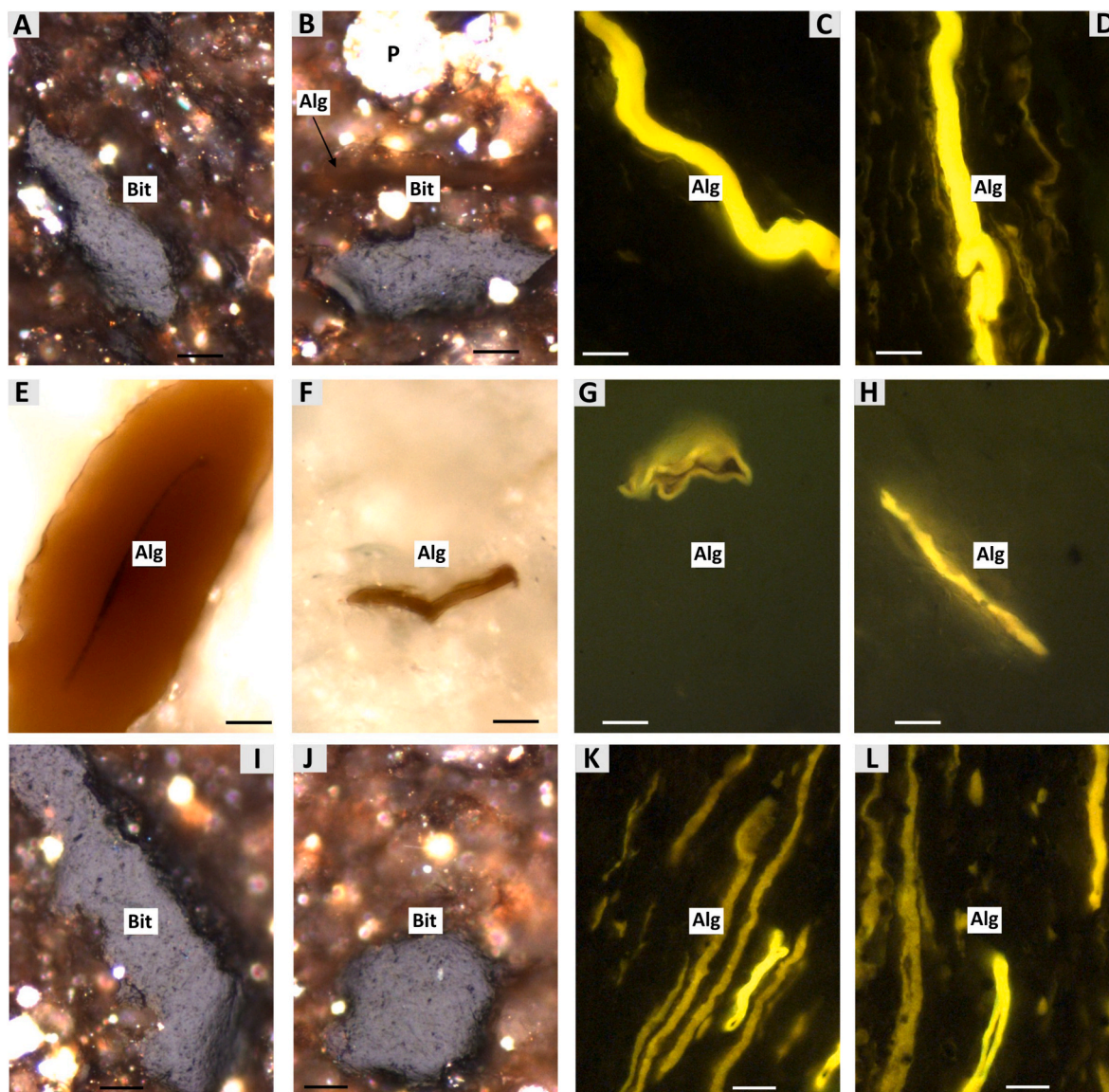


Fig. 15. Photomicrographs of dispersed organic matter from the 44,266 drill hole taken under reflected white light and fluorescence light sources. UV light excitation is at 465 nm; combined dichroic and barrier filter have a cut at 515 nm. The scale bar is 10 μm . Lachine Member at 434 m: (A–B) Bitumen BRo of 0.53% and 0.51%, respectively; P=Pyrite, (C–D) Alginite. Paxton Member at 440 m: (E–H) Alginite; note the central suture line in the thick-walled *Tasmanites* telalginite in (E). Norwood Member at 450 m: (I–J) Bitumen BRo of 0.52% and 0.55%, respectively, (K–L) Alginite.

oxygen deficiency conditions in bottom water (Lückge et al., 1999; Ercegovac and Kostic, 2006; Paction et al., 2011; Mansour et al., 2020a). The common incorporation of pyrite inclusions in the AOM particles also reveals enhanced reducing environments and accumulation under improved preservation potential of benthic microbial mats and planktonic organic matter (Tyson, 1995; Ercegovac and Kostic, 2006; Mansour et al., 2020b), which is consistent with enhanced euxinic conditions as evidenced from organic and inorganic geochemical investigations (Brown and Kenig, 2004; Formolo et al., 2014).

5.2.2. PFA-2

This palynofacies cluster occurs predominantly within the Paxton Member and is dominated by relatively moderate abundances of AOM and phytoclasts (Fig. 5). The average phytoclast particles in the PFA-2 reach up to 42.3% of total POM. They are dominated by opaque woody particles (avg. 26.5%), which comprise almost twice the number of translucent debris (avg. 15.8%, Fig. 6). Besides, the Opq:Trs ratio is slightly higher (avg. 5.3) in this palynofacies cluster compared to the PFA-1 (Fig. 7). The TOC content of this palynofacies is commonly less

than 2 wt%, except for two samples from the Lachine and Norwood members in the 60,134-drill hole, both of which have about 7.5 wt% (Fig. 7, Table 2). Therefore, the phytoclast composition, along with the Opq:Trs ratio of the PFA-2, suggest two possible interpretations. The first is related to the deposition of organic-lean samples of the PFA-2 in a slightly oxidizing proximal shelf environment, in which selective decomposition of organic components has occurred (Fig. 8, Tyson, 1995; Mansour et al., 2020c). This interpretation is further supported by the minor relative sea level fall triggered by phases of isostatic rebounds and compression associated with the Acadian Orogeny. The sea level fall enhanced the oxygenation level of the water column (Gutschick and Sandberg, 1991). This redox setting during deposition of the PFA-2 is consistent with significantly lower concentrations of TOC, Mo, U, and a low Mo/TOC ratio relative to the PFA-1, all indicating deposition under enhanced dysoxic conditions (Formolo et al., 2014). The second explanation refers to the two organic-rich samples, which are interpreted to have been deposited during enhanced water column productivity supported by minor fluvio-deltaic organic matter input and phytoclasts. Deposition of these two samples occurred in a slightly distal, oxygen

depleted inner neritic shelf environment (Fig. 8, Tyson, 1993, 1995; Pittet and Gorin, 1997; Mansour et al., 2020a, 2020b, 2020c; Xia et al., 2021). A long distance of transport is expected to oxidize/alter a high proportion of translucent phytoclasts into opaque wood particles. Our results are consistent with the small particle size of most counted phytoclasts, thus indicating deposition in distal marine settings (Fig. 8, Tyson, 1993, 1995; Pittet and Gorin, 1997), but slightly shallower than the settings of PFA-1.

According to the POM composition of this cluster, all samples plot in the palynofacies field VI in the APP ternary diagram (Tyson, 1993), indicating a Type II kerogen mainly of marine oil-prone organic matter (Fig. 5B). This field shows that the PFA-2 was deposited in a slightly shallower shelf, typically in an inner neritic sea environment compared to the distally deposited PFA-1 (Tyson, 1993, 1995). Additionally, the field indicates dysoxic conditions during the deposition of the Paxton Member that are consistent with diminished Mo, U, and a low Mo/TOC ratio (Formolo et al., 2014). Brown and Kenig (2004) observed significant bioturbated fabrics within the Paxton core samples, revealing deposition of this organic-lean member under an oxic-dysoxic water column.

5.2.3. Palynomorphs implication for paleoenvironmental reconstruction

The qualitative change in acritarchs and prasinophyte phycmata and their relative fluctuations can be used to reconstruct the proximal-distal trends of the shoreline (Fig. 7, e.g., Jacobson, 1979; Wicander and Playford, 1985; Li-chang and Wicander, 1988; Stricanne et al., 2004; Wicander and Playford, 2013). Prasinophyte-rich sediments (average ca. 70% of total palynomorphs content) are encountered in the Antrim Formation, particularly within the deepest well compared to moderate enrichment (avg. 52%) in the marginal wells. The above is indicative of low energy water and enhanced reducing conditions from the basin margin towards the deeper shelf environment. This is consistent with prevalent oxygen-depleted bottom water conditions, especially during deposition of the Norwood and Lachine members in the Michigan and Illinois basins (Brown and Kenig, 2004; Formolo et al., 2014). However, fluvio-deltaic settings cannot be excluded especially at the northern and southern margins of the Michigan Basin. Our assumption is based on the presence of minor signals of plant spores such as *Calamospora obtecta*, *Verrucosiporites* sp., *Punctatisporites* sp., and *Triletes* sp. in the two drill holes (44,266 and 48,772) on the Michigan Basin margin compared to their absence in the deeper 60,134-drill hole (Tyson, 1993, 1995). Further evidence of fluvio-deltaic input into the Michigan Basin during the Late Devonian Period was reported by Gutschick and Sandberg (1991).

Process-bearing acritarch genera such as *Michrhystridium* and *Unellium* are more frequent in areas of proximal, shallow marine environment compared to a distal shelf basin setting (Stricanne et al., 2004). *Michrhystridium* is the most abundant process-bearing genus in the Antrim Shale samples, but it is sparsely recorded in samples on the basin margin drill holes (44,266 and 48,772), whereas *Unellium* is reported only in the Paxton Member in the 48,772-drill hole (Fig. 8), strongly suggesting a distal neritic shelf condition. In contrast, the genus *Veryhachium* is interpreted to adapt and thrive in areas of open sea environments (Fig. 8) compared to *Leiosphaerid* class that reflects a marginal shallow water environment (Jacobson, 1979). Even though *Tasmanites* and *Leiosphaeridium* genera are the most common palynomorphs in the Antrim Shale Formation, they show significant oscillations that are consistent with the sea level transgressive-regressive phases. In the study samples, *Veryhachium* is reported only within the Upper Member at the basin depocenter with an upward decrease versus a significant increase in the *Leiosphaeridium* sp., and thus suggesting an inverse relationship between both categories and a shallowing up phase of the sea level. Similar palynomorphs assemblages of acritarchs and prasinophytes were recorded within the Upper Devonian sediments of the Mid-continent North America. Excluding the most abundant species of *Tasmanites* spp. and *Leiosphaeridia* spp., a widespread occurrence of acritarch and

prasinophyte species, such as *Cymatiosphaera chelina*, *C. parvicarina*, *C. ambotrocha*, *C. perimembrana*, *Muraticavea enteichia*, *Polyedryxium pharaone*, *Dictyotidium torosum*, *D. cf. craticulum*, *Comasphaeridium muscosum*, *Alocomurus compactus*, *L. deminutum*, *L. segregum*, *L. pelicanensis*, *Navifusa bacilla*, *Veryhachium arcarium*, *V. europaeum*, *V. trispinosum*, and *Unellium elongatum* among others, was reported. These species were reported in the Chagrin Shale in Ohio (Wicander, 1974; Molyneux et al., 1984), the Lime Creek Formation in Iowa (Wicander and Playford, 1985), the Antrim Shale Formation in Indiana (Wicander and Loeblich, 1977), and the Saverton Shale in the Illinois Basin (Wicander and Playford, 2013). These previous studies indicated that the Upper Devonian shale sediments were deposited under a low energy, slightly distal marine environment. Additionally, the close geographic proximity between the above sedimentary basins and the regional similarity between Late Devonian palynomorphs assemblages suggest widespread and similar water masses.

5.3. Antrim Shale source rock characterization

A preliminary assessment of the Antrim Shale source rock quality and quantity can be developed based on the measured TOC/Rock-Eval pyrolysis parameters, including Sh0, Sh1, Sh2, HI, OI, and T_{max} (Espitalié et al., 1985; Peters, 1986; Peters et al., 1994; Baskin, 1997; Carvajal-Ortiz and Gentzis, 2015). Most samples are rich in organic matter, with a few samples of the Upper and Norwood members from the 60,134-drill hole characterized by a good to very good organic richness. Unlike the black shale intervals of the Antrim Shale Formation, the gray shale of the Paxton Member (0.23–0.84 wt%, avg. 0.6 wt%) is dominated by poor to fair organic richness in the three drill holes (Fig. 7, Table 2).

The hydrocarbon generating potential (S_2) of the study samples in the Lachine, Norwood, and Upper members is generally excellent (11.5–116.5, avg. 43.5 mg HC/g rock), in contrast to the Paxton Member (0.6–5.4, avg. 2 mg HC/g rock), which shows poor to fair hydrocarbon potential (Fig. 7). Only two samples from the Upper Member and one sample from the Norwood Member in the 60,134-drill hole are characterized by an average S_2 value of 6.6 mg HC/g rock, pointing to a good hydrocarbon generation potential (Peters, 1986; Peters et al., 1994; Baskin, 1997; Carvajal-Ortiz and Gentzis, 2015).

The HI values display a wide range from 308 to 599 mg HC/g TOC (avg. 431 mg HC/g TOC) with the highest values reported from the Norwood and Lachine members (Fig. 7). These values indicate a kerogen Type II in the Antrim Shale Formation throughout the Michigan Basin, except for four samples in the Paxton Member. These samples are dominated by lower HI values (207–263 mg HC/g TOC), revealing a mixed Type II/III kerogen (Peters, 1986; Peters et al., 1994; Baskin, 1997; Carvajal-Ortiz and Gentzis, 2015). The former interpretation of kerogen types is also indicated by the plot of TOC and S_2 values (Fig. 9, Espitalié et al., 1985), where most samples plot in the field of oil-prone kerogen Type II that usually originates from marine-source organic matter. Additionally, some of the Paxton Member samples plot very close to the null point in the field of mixed Type II/III oil to gas prone kerogen (Fig. 9).

The degree of thermal maturity of preserved organic matter can be assessed based on the measured T_{max} values, the relationship of the Rock-Eval HI versus T_{max} (Fig. 10), and the calculated vitrinite reflectance values (%VRo-eq). It is highly advantageous to compare the measured values of T_{max} with vitrinite and bitumen reflectance since the former is influenced by several factors, including type of organic matter, diagenetic alteration overprint, and paleoenvironmental conditions (Peters, 1986; Carvajal-Ortiz and Gentzis, 2015). Overall, the T_{max} values of the Antrim Shale Formation are low to moderate, indicating that all samples are in the immature to early stage of oil window (Table 2). One sample from the Norwood Member in the 44,266-drill hole had the highest T_{max} value of 448 °C, indicating peak oil window stage (Peters, 1986; Peters et al., 1994; Baskin, 1997; Carvajal-Ortiz and

Gentzis, 2015). This interpretation is further supported by the HI and T_{max} cross-plot (Fig. 10, Espitalié et al., 1985), where all samples plot in the oil window field except for three samples from the organic-lean Paxton Member that plot in the immature field. However, a reverse relationship between depth variation and T_{max} values of most Paxton Member samples is noticed (i.e., samples at deeper depths in the 60, 134-drill hole are characterized by relatively lower T_{max} values (426–428 °C) and vice versa (Table 2). The same holds true for the %Vro-eq (0.82–0.70) and %BRo values (0.7–0.57) with increasing depth (Table 3). Few of the higher T_{max} values measured in the less mature Antrim Shale samples may be explained by differences in the source of the organic matter (organic facies), particularly when terrigenous. A similar observation was made by French et al. (2019) in the Permian Basin of Texas, who noted that the immature Pepper Shale/Woodbine mudstones that contain terrigenous organic matter have higher T_{max} than the immature Eagle Ford source rock encountered at similar depths that contains marine organic matter.

Vitrinite reflectance measurements on homogenous organic particles have been widely used to corroborate the Rock-Eval T_{max} from programmed pyrolysis (Carvajal-Ortiz and Gentzis, 2015, 2018; Petersen et al., 2020; Mansour et al., 2020a, 2020b; Xia et al., 2021). The measured %BRo and %Vro-eq values show a progressive increase in thermal maturity with respect to depth (Table 3), which is in a good agreement with the T_{max} results for the Upper and Lachine members. Although the Norwood Member exhibits inconsistent trends between T_{max} and %Vro-eq values with depth in the shallow drill holes, the liptinitic organic matter changes in color with depth from bright green to dull yellow and amber (Figs. 13–15). This fluorescence color change with depth in the deeper drill hole is consistent with the measured %Vro-eq values and shows a mature source rock compared to the relatively low maturity source rocks in the shallower drill holes at the basin margin. It further indicates that the change in color of the liptinite macerals is more reliable than T_{max} results in this particular situation.

The studied samples are characterized by high yield and excellent hydrocarbon potential, which show a potential to expel hydrocarbons. The analyzed samples have variable HI and TOC values, although the kerogen is mostly Type II. A preferential absorption of different compounds by kerogen and varying expulsion efficiencies are expected. Source rocks that have high TOC and HI values are anticipated to expel hydrocarbons earlier and at higher oil/gas ratios compared to those

having lower values. The reason being that source rocks with higher HI values (e.g., intervals in the Norwood and Lachine members) will likely retain, via absorption, a smaller fraction of generated liquids because their retention capacity will be reached at lower levels of thermal maturation (Sandvik et al., 1992). Furthermore, the composition of any expelled hydrocarbons is expected to be affected by their absorption within the kerogen structure. Based on experimental generation and expulsion studies (Sandvik et al., 1992), expelled hydrocarbons from the Antrim Shale source rock intervals will likely be enriched in saturated hydrocarbons, followed by aromatics and polar/NSO compounds as a result of selective absorption. Our interpretation is based on the relationship between the free hydrocarbon (Sh0+Sh1) and TOC content (Fig. 11), whereby most samples plot around the line of Oil Shows. These results suggest the ability of the Antrim Shale samples to expel and flow hydrocarbons. This can be further supported by the calculated oil saturation index (OSI) values (Jarvie et al., 2012). OSI must exceed 100 mg HC/g TOC for a formation to be able to flow hydrocarbons without fracture stimulation. For the Antrim Shale Formation, the average value of the OSI is 83.6 mg HC/g TOC, although, the OSI values for the Upper, Paxton and Norwood members exceed the threshold of 100 mg HC/g TOC (Table 2). It should be noted that expulsion efficiency is not governed by source rock organic richness (i.e., TOC), but by kerogen composition and the initial HI (H₁₀) of kerogen, with the latter playing an important role in controlling the expulsion process (Pepper, 1992). The present-day HI values in the Norwood and Lachine members are in the 320–600 mg HC/g TOC range (Table 2). By extrapolating from the T_{max} versus HI plot, the H₁₀ values of the Type II marine kerogen in these members were approximately 380–650 mg HC/g TOC when marginally mature to early mature (~0.55–0.60 %BRo). Based on the expulsion efficiency model of Pepper (1992), these source rocks can be considered as early and highly efficient hydrocarbon expellers.

The relationship between the PI and T_{max} values (Fig. 12) is commonly used to reveal the possibility of hydrocarbon expulsion. This cross-plot divides the Antrim Shale Formation into two groups. The first group belongs to the deepest drill hole (60,134), in which the kerogen is in the oil window stage. The second group is dominated by samples from the Upper, Norwood, and Lachine members within the shallow drill holes (44,266 and 48,772), in which the kerogen has a low level of hydrocarbon conversion (Fig. 12). Three samples from the Paxton Member in the 60,134-drill hole plot in the field of significantly rich Sh0+Sh1 content, likely related to hydrocarbon migration (Fig. 12).

Table 3

Organic petrography parameters of the Antrim Shale Samples. SD = Standard deviation, Br = Bitumen reflectance, Vro-Eq = equivalent vitrinite reflectance.

Well ID	Member	Depth (m)	Number of measurements	BR	SD	Vro- Eq	
				%		%	
44,266	Lachine	434	25	0.53	0.03	0.71	
	Paxton	440	1	0.67	N/A	0.8	
	Norwood	450	12	0.56	0.06	0.74	
60,134	Upper	457	25	0.59	0.05	0.75	
		982	6	0.56	0.05	0.73	
	Lachine	985	13	0.58	0.05	0.75	
		1009	5	0.63	0.02	0.77	
	Paxton	1018	10	0.58	0.04	0.74	
		1030	1	0.7	N/A	0.82	
	Norwood	1033	3	0.57	0.04	0.74	
		1040	23	0.68	0.05	0.81	
		1043	24	0.64	0.02	0.78	
		1049	9	0.7	0.06	0.82	
	48,772	Upper	515	31	0.51	0.07	0.7
			519	17	0.54	0.05	0.72
Lachine		545	26	0.6	0.05	0.76	
		557	3	0.6	0.01	0.76	
Norwood		564	32	0.62	0.06	0.77	
		569	10	0.54	0.03	0.72	

Vro was calculated from BRo using the equation of Liu et al. (2019) ($Vro = 0.5992 \times BRo + 0.3987$).

6. Conclusions

The Antrim Formation in the Michigan Basin contains a moderate amount of moderately to well-preserved prasinophyte phycomata and acritarchs that reveal a significant biostratigraphic correlation to nearby basins. The palynomorphs confirmed a late Frasnian age for the Norwood and Paxton members and an early Famennian age for the Lachine and Upper members. Statistical analysis of POM composition defined two palynofacies assemblages, both of which revealed deposition of the Antrim Shale in low energy, distal inner neritic shelf environment. Samples of the PFA-2 were slightly shallower and deposited under dysoxic conditions, unlike the PFA-1 that was deeper and deposited under severe anoxia. Higher organic richness in the Norwood, Lachine and Upper members (TOC up to 25.1 wt%, avg. 8.5 wt%) is associated with more reducing conditions, which is consistent with other Late Devonian-Early Mississippian Shales such as the Bakken Shale in the Williston Basin, Chattanooga Shale in the Appalachian Basin, the New Albany Shale in the Illinois Basin, and Exshaw Shale in the Western Canada Basin. This is also consistent with high concentration of Mo, U, Mo/TOC, and pyrite sulfur for the Norwood and Lachine members compared to depleted redox-sensitive elements within the organic-lean Paxton Member that belongs to the PFA-2, indicating varied redox conditions. Thin ash marker beds at top of the Lachine Member in the Michigan Basin underpin severe redox conditions that are consistent

with a Late Devonian extinction event. Thus, the regional change in relative sea level during the Frasnian-Famennian time resulted in a fluctuation of the degree of reducing conditions. Geochemical characterization indicated excellent hydrocarbon generating potential of kerogen Type II of marine oil-prone organic matter for the Norwood, Lachine and Upper members. This is in contrast to the organic-lean Paxton Member that contained a mixed Type II/III of oil/gas prone kerogen. Thermal maturity revealed that all samples are in the oil window, except for minor intervals of the Paxton Member that are in the immature stage. In addition, the higher maturity in the deeper drill hole at the basin center was confirmed by the weak dull yellow to brown fluorescence colors of the telalginite, whereas the telalginite in the two shallower drill holes had a very strong golden yellow fluorescence color. According to the Rock-Eval pyrolysis parameters, most of the Antrim Shale source rock layers showed a tendency to hydrocarbon flow without the need for fracture stimulation.

Author statement

To the editor in chief, Prof. Massimo Zecchin, I would like to indicate that all authors have made a significant contribution to produce the final version of this manuscript, from the first step to introduce a suitable idea with important contribution to science, sampling strategy, application procedures and analytical techniques, lab measurements, constructing observatory figures and charts, data analysis, interpreting and writing scientific parts, to submission and revision of the manuscript. On behalf of the authors, Ahmed Mansour.

Declaration of competing interest

The authors declare that they have no known competing financial interests or personal relationships that could have appeared to influence the work reported in this paper.

Acknowledgement

We thank Christa-Ch. Hofmann, the Institute of Paleontology, University of Vienna, for providing the microscopic unit to investigate the palynological and palynofacies composition of the studied samples during the post-doctoral visit of the first author. We also thank the Michigan Geological Repository for Research and Education (MGRRE) for providing access to the core and facilitating sampling. The manuscript benefitted from technical editing provided by the Central Michigan University Writing Center and Christopher Gentzis. The authors thank the journal associate editor Swapnan Kumar Sahoo and three anonymous reviewers for their constructive comments that improved the final version of the paper.

Appendix A. Supplementary data

Supplementary data to this article can be found online at <https://doi.org/10.1016/j.marpetgeo.2022.105683>.

References

- Adeyilola, A., Zakharova, N., Liu, K., Gentzis, T., Carvajal-Ortiz, H., Ocabalidet, S., 2022. Hydrocarbon potential and organofacies of the devonian Antrim shale, Michigan basin. *Int. J. Coal Geol.* 249, 103905.
- Algeo, T.J., Lyons, T.W., Blakey, R.C., Over, D.J., 2007. Hydrographic conditions of the Devonian–Carboniferous North American Seaway inferred from sedimentary Mo–TOC relationships. *Palaeogeogr. Palaeoclimatol. Palaeoecol.* 256 (3–4), 204–230.
- ASTM D7708-14, 2014. Standard Test Method for Microscopical Determination of the Reflectance of Vitrinite Dispersed in Sedimentary Rocks. ASTM International, West Conshohocken, PA. www.astm.org.
- Baskin, D.K., 1997. Atomic H/C ratio of kerogen as an estimate of thermal maturity and organic matter conversion. *AAPG Bull.* 81, 1437–1450.
- Batten, D.J., 1996. Chapter 7C Colonial Chlorococcales, 1. *AASP Found.*, pp. 191–203.
- Bharadwaj, D.C., Tiwari, R.S., Venkatachala, B.S., 1970. An upper devonian microflora from New Albany shale, Kentucky. *U.S.A. Palaeobot.* 19, 29–40.
- Boothroyd, J., 2012. Carboniferous Provenance Trends from Clastic Strata of the Michigan Basin [unpublished MS Thesis]. Michigan State University, East Lansing.
- Brown, T.C., Kenig, F., 2004. Water column structure during deposition of Middle Devonian–Lower Mississippian black and green/gray shales of the Illinois and Michigan Basins: a biomarker approach. *Palaeogeogr. Palaeoclimatol. Palaeoecol.* 215, 59–85.
- Calvert, S.E., Bustin, R.M., Ingall, E.D., 1996. Influence of water column anoxia and sediment supply on the burial and preservation of organic carbon in marine shales. *Geochem. Cosmochim. Acta* 60, 1577–1593.
- Carvajal-Ortiz, H., Gentzis, T., 2015. Critical considerations when assessing hydrocarbon plays using Rock-Eval pyrolysis and organic petrology data: data quality revisited. *Int. J. Coal Geol.* 152, 113–122.
- Carvajal-Ortiz, H., Gentzis, T., 2018. Geochemical screening of source rocks and reservoirs: the importance of using the proper analytical program. *Int. J. Coal Geol.* 190, 56–69.
- Curtis, J.B., 2002. Fractured shale-gas systems. *AAPG Bull.* 86 (11), 1921–1938.
- Decker, D., Coates, J.M.P., Wicks, D., 1992. Stratigraphy, gas occurrence, formation evaluation and fracture characterization of the Antrim Shale, Michigan basin. In: *Topical Report No. PB-95-104642/XAB*. Advanced Resources International, Inc. (Lakewood, CO, USA).
- Dellapenna, T.M., 1991. Sedimentological, Structural, and Organic Geochemical Controls on Natural Gas Occurrence in the Antrim Formation in Otsego County, Michigan. Unpublished Master Dissertation, Western Michigan University.
- Dorr, J.A., Eschman, D.F., 1970. *Geology of Michigan*. University of Michigan Press.
- East, J.A., Swezey, C.S., Repetski, J.E., Hayba, D.O., 2012. Thermal maturity map of Devonian shale in the Illinois, Michigan, and Appalachian basins of North America. *U.S. Geol. Surv. Sci. Invest. Map* 3214 (1).
- Ercegovac, M., Kostic, A., 2006. Organic facies and palynofacies: nomenclature, classification and applicability for petroleum source rock evaluation. *Int. J. Coal Geol.* 68, 70–78.
- Espitalié, J., Deroo, G., Marquis, F., 1985. La pyrolyse Rock-Eval et ses applications, vol. 40. *Revue Institut Français du Pétrole*, pp. 563–579. Partie 1.
- Ettensohn, F.R., 1995. Global and regional controls on the origin and burial of organic matter in Devonian–Mississippian black shales of North America. *Bull. -Houst. Geol. Soc.* 37, 12–17.
- French, K.L., Birdwell, J.E., Whidden, K.J., 2019. Geochemistry of a thermally immature Eagle Ford Group drill core in central Texas. *Org. Geochem.* 131, 19–33.
- Formolo, M.J., Riedinger, N., Gill, B.C., 2014. Geochemical evidence for euxinia during the Late Devonian extinction events in the Michigan Basin (U.S.A.). *Palaeogeogr. Palaeoclimatol. Palaeoecol.* 414, 146–154.
- Ghavidel-syooki, M., Owens, B., 2007. Palynostratigraphy and palaeogeography of the Padeha, Khosheyilagh, and Mobarak formations in the eastern Alborz Range (Kopet-Dagh region), northeastern Iran. *Rev. Micropaleontol.* 50, 129–144.
- Gilleaudeau, G.J., Algeo, T.J., Lyons, T.W., Bates, S., Anbar, A.D., 2021. Novel watermass reconstruction in the Early Mississippian Appalachian Seaway based on integrated proxy records of redox and salinity. *Earth Planet Sci. Lett.* 558, 116746.
- Gutschick, R.C., 1987. Devonian shelf-basin, Michigan Basin, Alpena, Michigan. *N. Centr. Sec. Geol. Soc. Am.: Boulder, Colorado, Geol. Soc. Am., Centen. Field Guide* 3, 297–302.
- Gutschick, R.C., Sandberg, C.A., 1991. Late Devonian history of Michigan basin. Early sedimentary evolution of the Michigan basin. *Geol. Soc. Am. Spec. Pap.* 256, 181–202.
- Hammer, Ø., Harper, D.A.T., Ryan, P.D., 2001. PAST: paleontological statistics software package for education and data analysis. *Palaeontol. Electron.* 4, 4–9.
- Harker, S.D., Sarjeant, W.A.S., Caldwell, W.G.E., 1990. Late Cretaceous (Campanian) organic-walled microplankton from the Interior Plains of Canada, Wyoming, and Texas: biostratigraphy, palaeontology, and palaeoenvironmental interpretation. *Palaeontology* 219, 1–243.
- Hashemi, H., Playford, G., 1998. Upper Devonian palynomorphs of the Shishtu Formation, Central Iran Basin, east-central Iran. *Palaeontograph. Abteilung B* 246, 115–212.
- Huysken, K.T., Wicander, R., Ettensohn, F.R., 1992. Palynology and biostratigraphy of selected Middle and Upper Devonian black-shale sections in Kentucky. *Mich. Acad.* 24, 355–368.
- Ingall, E.D., Bustin, R.M., Vancappellen, P., 1993. Influence of water column anoxia on the burial and preservation of carbon and phosphorus in marine shales. *Geochem. Cosmochim. Acta* 57, 303–316.
- ISO 7404-2, 2009. Methods for the petrographic analysis of coal – Part 2: methods of preparing coal samples. In: *International Organization for Standardization. ISO 7404-2: 2009(en)*. www.iso.org/standard/42798.html.
- ISO 7404-5, 2009. In: *Methods for the Petrographic Analysis of Coal – Part 5: Methods of Determining Microscopically the Reflectance of Vitrinite*. International Organization for Standardization, Geneva, Switzerland, p. 14.
- Jacobson, S.R., 1979. Acritarchs as palaeoenvironmental indicators in the Middle and Upper Ordovician Rocks from Kentucky, Ohio and New York. *J. Paleontol.* 53, 1197–1212.
- Jarvie, D.M., Jarvie, B.M., Weldon, W.D., Maende, A., 2012. Components and Processes Impacting Production Success from Unconventional Shale Resource Systems. *Search and Discovery. Article #40908*.
- Johnson, J.G., 1970. Taghanic Onlap and the end of the North American Devonian provinciality. *Geol. Soc. Am. Bull.* 81, 2077–2106.
- Langford, F.F., Blanc-Valleron, M.-M., 1990. Interpreting Rock-Eval pyrolysis data using graphs of pyrolyzable hydrocarbons vs. Total Organic Carbon. *AAPG Bull.* 74, 799–804.

- Leventhal, J.S., 1987. Carbon and sulfur relationships in Devonian shales from the Appalachian Basin as an indicator of environment of deposition. *Am. J. Sci.* 287, 33–49.
- Li-chang, L., Wicander, R., 1988. Upper Devonian acritarchs and spores from the Hongguleleng Formation, Hefeng district in Xinjiang, China. *Rev. Espanola Micropaleontol.* 20, 109–148.
- Liu, B., Mastalerz, M., Schieber, J., Teng, J., 2020. Association of uranium with macerals in marine black shales: Insights from the Upper Devonian New Albany Shale, Illinois Basin. *Int. J. Coal Geol.* 217, 103351.
- Liu, B., Schieber, J., Mastalerz, M., Teng, J., 2019. Organic matter content and type variation in the sequence stratigraphic context of the Upper Devonian New Albany Shale, Illinois Basin. *Sediment. Geol.* 383, 101–120.
- Lückge, A., Ercegovac, M., Strauss, H., Littke, R., 1999. Early diagenetic alteration of organic matter by sulfate reduction in Quaternary sediments from the northeastern Arabian Sea. *Mar. Geol.* 158, 1–13.
- Mansour, A., Gentzis, T., Carvajal-Ortiz, H., Tahoun, S.S., Elewa, A.M.T., Mohamed, O., 2020b. Source rock evaluation of the Cenomanian Raha Formation, Bakr oil field, Gulf of Suez, Egypt: Observations from palynofacies, RGB-based spore morphology microscopy, and organic geochemistry. *Mar. Petrol. Geol.* 122, 104661.
- Mansour, A., Gerslova, E., Sykorova, I., Vörös, D., 2020a. Hydrocarbon potential and depositional paleoenvironment of a Middle Jurassic succession in the Falak-21 well, Shushan Basin, Egypt: Integrated palynological, geochemical and organic petrographic approach. *Int. J. Coal Geol.* 219, 103374.
- Mansour, A., Wagreich, M., Gentzis, T., Oucbalidet, S., Tahoun, S.S., Elewa, A.M.T., 2020c. Depositional and organic carbon-controlled regimes during the Coniacian-Santonian event: First results from the southern Tethys (Egypt). *Mar. Petrol. Geol.* 115, 104285.
- Martini, A.M., Walter, L.M., Budai, J.M., Ku, T.C., Kaiser, C.J., Schoell, M., 1998. Genetic and temporal relations between formation waters and biogenic methane: Upper Devonian Antrim Shale, Michigan Basin, USA. *Geochem. Cosmochim. Acta* 62 (10), 1699–1720.
- Matthews, R.D., 1993. Review and revision of the Devonian-Mississippian stratigraphy in the Michigan Basin. *US Geol. Surv. Bull. Rep.*: B 1909 D1–D85.
- Mendonça Filho, J.G., Menezes, T.R., Mendonça, J.O., Oliveira, A.D., Silva, T.F., Rondon, N.F., Da Silva, F.S., 2012. Organic facies: palynofacies and organic geochemistry approaches. In: Panagiotaras, D. (Ed.), *Geochemistry—Earth's System Processes*. InTech, pp. 211–248.
- McIntosh, J.C., Walter, L.M., Martini, A.M., 2004. Extensive microbial modification of formation water geochemistry: Case study from a Midcontinent sedimentary basin, United States. *Geol. Soc. Am. Bull.* 116 (5–6), 743–759.
- Molyneux, S.G., Manger, W.L., Owens, B., 1984. Preliminary account of Late Devonian palynomorph assemblages from the Bedford Shale and Berea Sandstone Formations of central Ohio, U.S.A. *J. Micropaleontol.* 3, 41–51.
- Nunn, J.A., Sleep, N.H., Moore, W.E., 1984. Thermal subsidence and generation of hydrocarbons in Michigan Basin. *AAPG Bull.* 68 (3), 296–315.
- Oucbalidet, S.G., Rimmer, S.M., Conder, J.A., 2018. Redox conditions associated with organic carbon accumulation in the Late Devonian New Albany Shale, west-central Kentucky, Illinois Basin. *Int. J. Coal Geol.* 190, 42–55.
- Over, D.J., 2002. The Frasnian/Famennian boundary in central and eastern United States. *Palaeogeogr. Palaeoclimatol. Palaeoecol.* 181, 153–169.
- Pacton, M., Gorin, G.E., Vasconcelos, C., 2011. Amorphous organic matter — experimental data on formation and the role of microbes. *Rev. Palaeobot. Palynol.* 166, 253–267.
- Pepper, A.S., 1992. Estimating the petroleum expulsion behavior of source rocks: a novel quantitative approach. In: England, W.A., Fleet, A.J. (Eds.), *Petroleum Migration*, vol. 59. *Geol. Soc., Spec. Pub.*, pp. 9–31.
- Pereira, Z., Matos, J., Fernandes, P., Oliveira, J.T., 2008. Palynostratigraphy and Systematic Palynology of the Devonian and Carboniferous Successions of the South Portuguese Zone, Portugal, vol. 34. *Memorias Geologicas do Instituto Nacional de Engenharia, Tecnologia e Inovação*, pp. 1–181.
- Peters, K.E., 1986. Guidelines for evaluating petroleum source rock using programmed pyrolysis. *AAPG Bull.* 70, 318–329.
- Peters, K.E., Cassa, M.R., Magoon, L.B., Dow, W.G., 1994. Applied source rock geochemistry. In: *The Petroleum System - from Source to Trap*. *AAPG Memoirs*, pp. 93–120.
- Petersen, H.I., Sanei, H., Gelin, F., Loustaunau, E., Despujols, V., 2020. Kerogen composition and maturity assessment of a solid bitumen-rich and vitrinite-lean shale: Insights from the Upper Jurassic Vaca Muerta shale, Argentina. *Int. J. Coal Geol.* 229, 103575.
- Pittet, B., Gorin, E., 1997. Distribution of sedimentary organic matter in a mixed carbonate-siliciclastic platform environment: Oxfordian of the Swiss Jura Mountains. *Sedimentology* 44, 915–937.
- Playford, G., 1981. Late Devonian acritarchs from the Gneudna Formation in the western Carnarvon Basin, Western Australia. *Geobios* 14, 145–171.
- Powell, T.G., Creaney, S., Snowdon, L.R., 1982. Limitations of use of organic petrographic techniques for identification of petroleum source rocks. *Am. Assoc. Petrol. Geol. Bull.* 66, 430–435.
- Quinlan, G.M., Beaumont, C., 1984. Appalachian thrusting, lithospheric flexure, and the Paleozoic stratigraphy of the Eastern Interior of North America. *Can. J. Earth Sci.* 21 (9), 973–996.
- Rimmer, S.M., 2004. Geochemical paleoredox indicators in Devonian–Mississippian black shales, central Appalachian Basin (USA). *Chem. Geol.* 206 (3–4), 373–391.
- Rimmer, S.M., Thompson, J.A., Goodnight, S.A., Robl, T.L., 2004. Multiple controls on the preservation of organic matter in Devonian–Mississippian marine black shales: geochemical and petrographic evidence. *Palaeogeogr. Palaeoclimatol. Palaeoecol.* 215, 125–154.
- Romero-Sarmiento, M.F., Pillot, D., Letort, G., Lamoureux-Var, V., Beaumont, V., Huc, A.-Y., Garcia, B., 2014. New Rock-Eval method for characterization of shale plays. In: 14th Latin American Congress on Organic Geochemistry (ALAGO). Buzios, Rio de Janeiro – Brazil.
- Romero-Sarmiento, M.F., Pillot, D., Letort, G., Lamoureux-Var, V., Beaumont, V., Huc, A. Y., Garcia, B., 2015. New Rock-Eval method for characterization of unconventional shale resource systems. *Oil Gas Sci. Technol. Rev. Inst. Fr. Pet. Energ. Nouv.* 71, 1–9.
- Root, S., Onasch, C.M., 1999. Structure and tectonic evolution of the transitional region between the central Appalachian foreland and interior cratonic basins. *Tectonophysics* 305 (1–3), 205–223.
- Rullkötter, J., Marzi, R., Meyers, P.A., 1992. Biological markers in Paleozoic sedimentary rocks and crude oils from the Michigan Basin: Reassessment of sources and thermal history of organic matter. In: *Early Organic Evolution*. Springer, Berlin, Heidelberg, pp. 324–335.
- Sandvik, E.I., Young, W.A., Curry, D.J., 1992. Expulsion from hydrocarbon sources: the role of organic absorption. *Org. Geochem.* 19, 77–87.
- Sanei, H., 2020. Genesis of solid bitumen. *Sci. Rep.* 10, 15595. <https://doi.org/10.1038/s41598-020-72692-2>.
- Schieber, J., Baird, G., 2001. On the origin and significance of pyrite spheres in Devonian black shales of North America. *J. Sediment. Res.* 71, 155–166.
- Song, Y., Gilleaudeau, G.J., Algeo, T.J., Over, D.J., Lyons, T.W., Anbar, A.D., Xie, S., 2021. Biomarker evidence of algal-microbial community changes linked to redox and salinity variation, Upper Devonian Chattanooga Shale (Tennessee, USA). *GSA Bull.* 133 (1–2), 409–424.
- Stricanne, L., Munneke, A., Pross, J., Servais, T., 2004. Acritarch distribution along an inshore-offshore transect in the Gorstian (lower Ludlow) of Gotland, Sweden. *Rev. Palaeobot. Palynol.* 130, 195–216.
- Swezey, C.S., 2008. Regional Stratigraphy and Petroleum Systems of the Michigan Basin. North America: U.S. Geol. Sur. Sci. Invest. Map 2978, 1 sheet, available at: <http://pubs.usgs.gov/sim/2978/>.
- Tyson, R.V., 1993. Palynofacies analysis. In: Jenkins, D.G. (Ed.), *Applied Micropaleontology*. Kluwer Acad. Publ, Netherlands, pp. 153–191.
- Tyson, R.V., 1995. *Sedimentary Organic Matter: Organic Facies and Palynofacies*. Chapman & Hall, London, p. 615.
- Tyson, R.V., 2001. Sedimentation rate, dilution, preservation and total organic carbon: some results of a modeling study. *Org. Geochem.* 32, 333–339.
- Venkatachala, B.S., 1981. Differentiation of amorphous organic types in sediments. In: Brooks, J. (Ed.), *Organic Maturation Studies and Fossil Fuel Exploration*. Academic Press, London, pp. 177–200.
- Wei, L., Wang, Y., Mastalerz, M., 2016. Comparative optical properties of vitrinite and other macerals from Upper Devonian–Lower Mississippian New Albany Shale: implications for thermal maturity. *Int. J. Coal Geol.* 168, 222–236.
- Werne, J.P., Sageman, B.B., Lyons, T.W., Hollander, D.J., 2002. An integrated assessment of a “type euxinic” deposit: evidence for multiple controls on black shale deposition in the Middle Devonian Oatka Creek Formation. *Am. J. Sci.* 302, 110–143.
- Wicander, E.R., 1974. Upper Devonian-Lower Mississippian acritarchs and prasinophyceyan algae from Ohio, U.S.A. *Palaeontographica*, bt B 148, 9–43.
- Wicander, E.R., 1975. Fluctuations in a Late Devonian-Early Mississippian phytoplankton flora of Ohio. U.S.A. *Palaeogeogr. Palaeoclimat. Palaeoecol.* 17, 89–108.
- Wicander, E.R., 1983. A catalog and biostratigraphic distribution of North American Devonian acritarchs. *Am. Assoc. Stratigr. Palynol. Contrib. Ser.* 10, 1–133.
- Wicander, E.R., Loeblich Jr., A.R., 1977. Organic-walled microphytoplankton and its stratigraphic significance from the Upper Devonian Antrim Shale, Indiana, U.S.A. *Palaeontogr. Abteilung B* 160, 129–165.
- Wicander, R., Playford, G., 1985. Acritarchs and spores from the Upper Devonian Lime Creek Formation, Iowa, U.S.A. *Micropaleontology* 31, 97–138.
- Wicander, R., Playford, G., 2013. Marine and terrestrial palynofloras from transitional Devonian-Mississippian strata, Illinois Basin. U.S.A. *Bol. Geol. Miner.* 124 (4), 589–637.
- Winslow, M.R., 1962. Plant spores and other microfossils from Upper Devonian and Lower Mississippian rocks of Ohio. In: *U.S. Geol. Sur., Professional Paper*, vol. 364, pp. 1–93.
- Wood, G.D., Gabriel, A.M., Lawson, J.C., 1996. Chapter 3. Palynological techniques—processing and microscopy. In: Jansonius, J., McGregor, D.C. (Eds.), *Palynology: Principles and Applications*, vol. 1. American Association of Stratigraphic Palynologists Foundation, Dallas, TX, pp. 29–50.
- Xia, G., Mansour, A., Gentzis, T., Li, G., Carvajal-Ortiz, H., Oucbalidet, S., Yi, F., Yun, C., Yi, H., 2021. Depositional paleoenvironment and source rock characterization across the Toarcian Oceanic Anoxic Event from the eastern Tethys, Tibet, SW China. *Int. J. Coal Geol.* 243, 103780.
- Ziegler, W., Sandberg, C.A., 1990. The Late Devonian standard conodont zonation. *Cour. Forschungsinst. Senckenberg* 121, 115.